Aquatic Geochemistry (2025) 31:5
https://doi.org/10.1007/s10498-025-09439-w

ORIGINAL ARTICLE

Assessing Silicate Catchment Dynamics of the Oplotnica River (Slovenia) Through Stable Carbon and Nitrogen Isotopes

Tjaša Kanduč[1] · **Mirijam Vrabec**[2] · **Timotej Verbovšek**[2] · **Jennifer McIntosh**[3] · **Daniel Žlindra**[4] · **Urša Vilhar**[4]

Received: 9 January 2025 / Accepted: 26 March 2025 / Published online: 25 April 2025

Abstract

This study investigated the sources of carbon and nitrogen in a small, silicate-dominated catchment (Oplotnica River, Pohorje, Slovenia) with two creeks, Lukanjski and Javorski, from 2012 to 2014. Additionally, carbon and nitrogen cycling in soil profiles was studied at Javorski Creek. Isotopic analyses of river water, particulates, and sediments provided a more holistic view of the sources of carbon and nitrogen, weathering contributions, and the evasion or sequestration of CO_2 in the atmosphere within the catchments. The weathering of rocks, such as granodiorite and quartz diorite, influences water geochemistry. The Oplotnica River and its tributaries were characterized by the ion composition: $Na^+ > Ca^{2+} > Mg^{2+} > K^+$ and $HCO_3^- > SO_4^{2-} > Cl^- > NO_3^-$. Partial pressure of CO_2 concentrations in river and creeks ranged from 1.1 to 13.4 times that of atmospheric pressure, representing a source of CO_2 to the atmosphere. The carbon isotope value of dissolved inorganic carbon ($\delta^{13}C_{DIC}$) ranged from −9.8 to −1.4‰ in river, while in the creeks, it ranged from −26.1 to −4.7‰, reflecting the degradation of organic matter and exchange with the atmosphere. The intensity of bicarbonate weathering for the Oplotnica River at its gauging station was 10.4 mmol/(l·km^2·s), characteristic of silicate watersheds. The isotopic composition of carbon ($\delta^{13}C$) and nitrogen ($\delta^{15}N$) in river sediments reflects values typical of soil and temperate (C3) plants. This study is significant on both local and global levels, as it addresses the contribution of weathering rates and the release of CO_2 to the atmosphere from small silicate watersheds.

Keywords River systems · Silicate catchment · Water–soil interactions · Stable isotopes · Weathering intensity · Oplotnica River

1 Introduction

Atmospheric and soil CO_2 absorption processes are fundamental in moderating Earth's climate by facilitating the movement of CO_2 from the atmosphere and soil into marine environments (Walker et al. 1981; Berner et al. 1983). Rivers play a pivotal role in the global carbon cycle, acting as conduits that interconnect atmospheric, terrestrial, and

---

Extended author information available on the last page of the article oceanic carbon reservoirs. Global estimates indicate that approximately 1.8×10^{15} gC of CO_2 degasses annually from rivers, with these data derived from studies on the world's largest river systems (Raymond et al. 2013). Dissolved carbon is the primary contributor to this degassing, accounting for 60% of the total, with dissolved inorganic carbon (DIC) representing 37% and dissolved organic carbon (DOC) making up 23% (Ludwig et al. 1996a, b). DIC in rivers generally consists of CO_2(aq), HCO_3^-(aq), and CO_3^{2-}(aq), and its concentration depends on factors such as pH, pCO_2, and water temperature. Within the pH range of 6.0–8.2, bicarbonate (HCO_3^-) predominates (Stumm and Morgan 1981). Furthermore, weathering processes significantly contribute to riverine dissolved loads, with silicate weathering accounting for 45% of the total loads in global rivers (Gaillardet et al. 1999). To further understand the interplay between rock weathering and carbon cycling, small tropical river basins dominated by crystalline silicate rocks have been examined. Research has highlighted that, even in silicate catchments, carbonate weathering and the decomposition of organic matter are integral to the riverine carbon cycle, contributing as much as 60% to the DIC pool (Senarathne et al. 2024).

The stable isotopic composition of dissolved inorganic carbon ($\delta^{13}C_{DIC}$) is a reliable indicator for identifying the sources of DIC, whether they are of natural origin or linked to human activities. This is because $\delta^{13}C_{DIC}$ signatures vary depending on the source, making it possible to differentiate between them (Atekwana and Fonyuy 2009; Zou 2016; Juhlke et al. 2019; Krusche et al. 2002; Wang et al. 2019; Yang et al. 1996). Researchers have employed $\delta^{13}C_{DIC}$ data to study various processes such as carbon assimilation during photosynthesis (Tomazini da Conceiçao et al. 2024), water loss through evapotranspiration (Atekwana et al. 2016), and the interactions between sulfuric acid and acid mine drainage (Fonyuy and Atekwana 2008). Additionally, $\delta^{13}C_{DIC}$ analysis has been instrumental in examining the breakdown of organic matter and the dissolution of carbonate minerals. These mechanisms have been explored across different environments, including acid-impacted areas and natural systems (Kanduč et al. 2007a; Kanduč et al. 2014; Kanduč et al. 2023; Porowska 2015). This isotopic approach continues to be a key tool for understanding the complexities of carbon cycling.

Stable carbon ($\delta^{13}C$) and nitrogen ($\delta^{15}N$) isotopic techniques are extensively used to investigate the sources and fate of suspended particulate organic matter (SPOM) and sediment organic matter (SOM) in aquatic systems (Ren et al. 2024). Both SPOM and SOM derive from biological sources and external inputs (Derrien et al. 2018; Rahman et al. 2021). Typically, $\delta^{13}C$, $\delta^{15}N$, and carbon/nitrogen (C/N) ratios vary among these different sources (Guo et al. 2020; Huang et al. 2020). $\delta^{13}C$ has been shown to be useful for identifying organic matter (OM) in aquatic environments, as it is influenced by several factors, such as water chemistry, initial productivity, hydrological characteristics of the watershed, and regional environmental conditions (Li et al. 2020). However, $\delta^{13}C$ analyses alone often cannot fully distinguish between OM sources in aquatic systems. Given the complexity of nitrogen's geochemical cycle, with various nitrogen components involved, $\delta^{15}N$ alone also has limitations for source identification (Li et al. 2020). C/N ratios, on the other hand, directly correlate with the quantity and type of OM from different sources, making them effective indicators of OM composition (Ogawa et al. 2021).

The dynamics of DIC and $\delta^{13}C_{DIC}$ in watersheds with diverse geology, climate, and land use have been examined in both recent and past studies worldwide (Kanduč et al. 2007a, b; Kanduč et al. 2023; Tomazini et al. 2024; Tian et al. 2019). However, there is a lack of stable isotope data on carbon and nitrogen in silicate catchments across Europe. Previous isotopic analyses indicate that the CO_2 in these regions is relatively young, and no significant age difference in soil CO_2 has been observed above either carbonate or non-carbonate bedrock (Ogrinc et al. 2016; Krajnc et al. 2016).

This study aimed to trace the $\delta^{13}C_{DIC}$ and the isotopic composition of carbon in particulate organic matter ($\delta^{13}C_{POM}$) over time and space in the Oplotnica River's silicate catchment area during 2012–2014. Using carbon and nitrogen isotope data, we sought to determine the sources of DIC and assess major biogeochemical processes. We hypothesized that two primary factors influence $\delta^{13}C_{DIC}$ in silicate catchment waters: equilibration with atmospheric CO_2 and the degradation of organic matter (OM). To identify the origin of DIC, we calculated fractionation lines and performed mass balance calculations to assess the contributions of atmospheric CO_2 and OM degradation. Additionally, we calculated evasion and weathering fluxes and compared these with global data. To investigate soil degradation and the origin of suspended particulate organic matter (SPOM), we analyzed sediments (C/N, $\delta^{13}C$, and $\delta^{15}N$) from Javorski Creek 1 at the Tratice sampling location (JC1 s). This analysis also helped determine the source of carbon in SPOM and the origin of carbon and nitrogen in particulate matter.

1.1 Catchment Characteristics

The Oplotnica River's catchment is located in the northeastern part of Slovenia, in the southeastern part of Pohorje Mountains, bordering the Pannonian Basin. Its geology is characterized by eclogite facies metamorphic rocks, primarily by gneisses and micaschists of Late Cretaceous age (Thöni 2002; Janäk et al. 2009). Metapelitic country rocks in this area enclose numerous lenses of eclogites, partly transformed to amphibolites, marbles and quartzites (Fig. 1, Fig. 2). During the Miocene, an igneous body of granodioritic composition was intruded into the metamorphic rocks (Altherr et al. 1995; Fodor et al. 2008; Trajanova et al. 2008) followed by numerous pegmatite dikes (Uher et al. 2014). A smaller body of quartz diorite near Oplotnica River formed prior to granodioritic intrusion and was later on mixed and mingled with its silicate host (Poli et al. 2020).

The Oplotnica River's catchment area (Fig. 1) covers approximately 52 km^2. This river basin is part of the larger Drava River basin. The Oplotnica River originates in Pohorje, near Rogla, and is 28 km long. It flows past Osankarica, Oplotnica, and Tepanje and joins at Dravinja near Žiče. The Oplotnica River is equipped with a gauging station at Perovec that has the catchment area of approximately 57.1 km^2 (Lavtar et al. 2020). This gauging station began operation in 2017. Between 2009 and 2017, no gauging station was operating in the Oplotnica River.

In the Oplotnica municipality area, we find all three groups of rocks based on their formation: igneous rocks on the extreme northern edge, metamorphic rocks in the northern half (hilly and mountainous part), and sedimentary rocks in the southern half (plain part) of the municipality (Fig. 1).

Headwaters of Javorski (approximal length of 7 km) and Lukanjski (approximal length of 5 km) creeks are composed of granodiorite and quartz diorite (Figs. 1, 2). In Cezlak, there is an active granodiorite quarry and an abandoned micaschist quarry and an abandoned quartz diorite quarry.

The southern half of the Oplotnica municipality area is composed of the youngest sedimentary rocks, which were deposited in the past by rivers and today by streams flowing from Pohorje. In the plain part of the municipality, proluvium and sandy clay and clayey gravel alternate. Proluvium appears directly along the lower parts of stream flows and in a

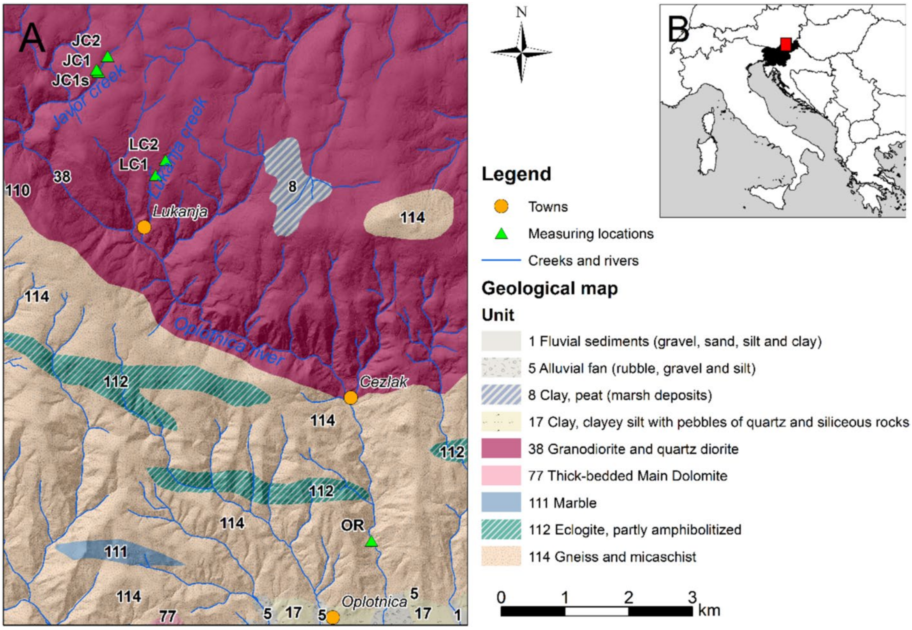

Fig. 1 Geological characteristics of sampling locations: JC1—Javorski creek downstream, JC1 s—soil profiles at Tratice I, Tratice II, Tratice III, JC2—Javorski creek upstream, LC1—Lukanjski creek downstream, LC2—Lukanjski creek upstream, OR—Oplotnica River. Modified after the Basic Geological Map 1:100,000, sheet L33-55 Slovenj Gradec (Mioč and Žnidarčič 1977)

narrow transitional band where the hills transition into the plain. Clay and gravel appear in larger patches in the remaining parts of the Oplotnica field (Mioč 1978).

In the past, the Oplotnica River was an extremely important source of water power, as in its upper course above Oplotnica, it powered more than 30 sawmills and small mills. Alongside them, small dams were built, which played an important role in retaining gravel and floodwaters. By the end of the nineteenth century, a quarry was opened near Cezlak, and for its needs, a small hydroelectric plant was built on the side tributary Oplotniščica, along with an industrial railway running through the gorge down to Oplotnica. Today, four small hydroelectric plants operate on the stream, with capacities ranging from 700 to 1400 kW.

The vegetation of the catchment area consists of sub-Alpine mixed deciduous–coniferous forests with prevailing tree species Norway spruce *Picea abies* (L. Karst) and European beech *Fagus sylvatica (L.)* (Vilhar et al. 2016).

The upper part of the watershed above Cezlak is included in the Natura 2000 protected area (Pohorje) (https://gis.arso.gov.si/atlasokolja/profile.aspx?id=Atlas_Okolja_AXL@Arso).

2 Materials and Methods

2.1 Sampling Protocols and Field Measurements

Surface water sampling was performed from September 2012 to June 2014 (Supplementary material—SM) at three locations: Lukanjski Creek (two locations: upstream and

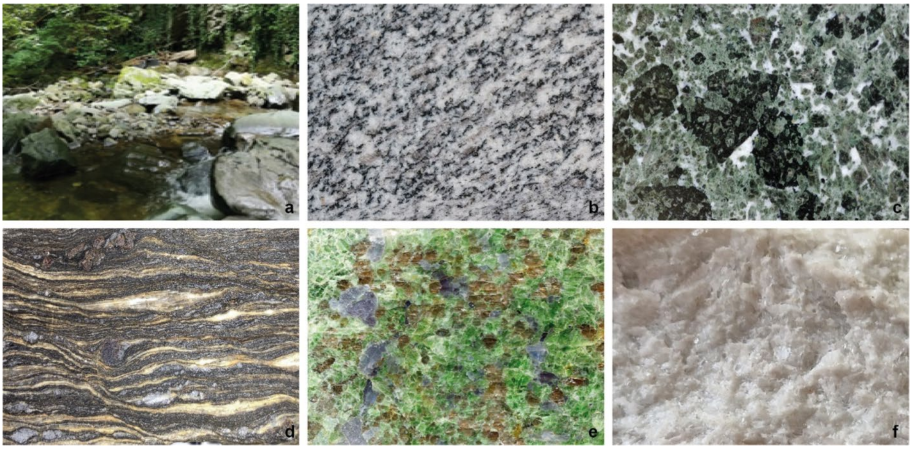

Fig. 2 Oplotnica River at Koritno and close-ups of representative igneous and metamorphic rocks from the silicate catchment area near sampling location OR. (**a**) General conditions in the creeks. (**b**) Granodiorite with white plagioclase, transparent quartz, pinkish potassium feldspars and black Fe–Mg minerals, mostly biotite and seldom amphibole. (**c**) Quartz diorite with white plagioclase, grayish transparent quartz and light green pyroxene which is replaced with dark green amphibole in typical uralitic texture. (**d**) Gneiss with big porphyroclasts of red garnet and white feldspars in a dark matrix composed mostly of micas, plagioclases, quartz and sometimes kianite. (**e**) Eclogite with red pyrope (garnet) and green omphacite (pyroxene), together with large blue kyanite. (**f**) Typical calcitic marble from Pohorje is coarse grained and very pure, with almost no non-carbonate minerals. The long rim of the figure equals 6 cm

downstream), Javorski Creek (two locations: upstream and downstream), and Oplotnica River (Fig. 1).

Discharge measurements from both Javorski and Lukanjski Creek were carried out with a metal Parshall flume during the period from May 21, 2008, to February 24, 2014. The design of the Parshall flume is standardized in accordance with ASTM D1941, ISO 9826:1992, and JIS B7553-1993. The discharge level and water temperature were measured with an automatic measuring device (HOBO Water Level Logger (13 ft) U20L-04) at 15-min intervals and manually recorded at regular monthly intervals for a reference. The discharge of free-flowing water at the Parshall flume was calculated using the general relationship between the flow rate (Q) and the height of the water at the measuring point (H) (Brouwer et al. 1985):

$$\mathrm{Q} = \mathrm{C} * \ \mathrm{H}^{n} \tag{1}$$

where n is a coefficient depending on the size of the flume.

The coefficients C and n are determined experimentally by calibrating the Parshall flume with respect to the flume throat width and can be found in the literature (USDI 2001). In our case, the throat width is 0.1524 m (6 in), so C equals 2.06 and n equals 1.58 (Vilhar et al. 2015). Measured water T and calculated Q values at 15-min intervals were aggregated into average discharge ($\mathrm{m}^3\ \mathrm{s}^{-1}$) for the year 2017.

However, no gauging station was operated at the Oplotnica River from 2009 to 2017; therefore, Q data for the Oplotnica River were provided from the 2017 hydrological year at the Perovec gauging location by Slovenian Environmental Agency (SEA).

For the chemical analyses, the samples were collected in HDPE bottles and brought back to the Laboratory of Forest Ecology of the Slovenian Forestry Institute for filtration and analysis, as described below.

Samples for $\delta^{13}C_{DIC}$ analyses were stored in glass serum bottles, filled without headspace, and sealed with septa caps. For stable carbon isotope analysis of particulate organic carbon ($\delta^{13}C_{POC}$) and particulate nitrogen ($\delta^{15}N$), samples were collected in three 1L LDPE bottles, following the method of Schuster and Reddy (2005). The samples of leaf and needle of the most characteristic plants (*Picea abies*, *Fagus sylvatica*) of catchment area were collected at Javorski creek in plastic bags for isotopic composition of carbon and nitrogen. Soil profiles were dug and pedologically described. Sediments for sieve analyses, C/N analyses, $\delta^{13}C$ and $\delta^{15}N$ analyses were collected in plastic bags.

2.2 Laboratory Analyses

Water analyses were conducted on a regular basis as the samples arrived. No pretreatment was used for pH (ISO 10523 2008), EC and alkalinity measurements. Conductivity was measured with the Metrohm (Metrohm AG, Herisau, Switzerland) Pt1000 electroconductivity electrode and Metrohm 712 Conductometer (ISO 7888 1985). Metrohm low ionic strength pH glass electrode was used for measuring pH. The HCO_3^- was measured as alkalinity (Double end-point titration, pH = 4.5, 4.2) with Metrohm pH electrode in combination with titrator Metrohm 702 SM Titrino using 0.01 M HCl as a titrant (ISO 9963–11994). All samples were analyzed automatically with the Metrohm 778 Sample Processor. All devices were controlled by Metrohm Tiamo™ 1.0 software.

Samples for cations (Ca^{2+}, Mg^{2+}, K^+, Na^+) and anions (SO_4^{2-}, Cl^-, NO_3^-) were first filtered through 0.45-µm acetate cellulose filters and then analyzed on an Ion chromatography Metrohm modular system consisting of a 762 IC Interface, 732 IC Detector, 820 IC Separation Center, 709 IC Pump, 752 Pump Unit and 766 IC Sample Processor (ISO 10304-1 2007, ISO 14911 1998). For cation analysis, a Metrosep C4-150/4.0 column was used and no suppression was applied. For anion analysis, a Metrosep A Supp 5–150/4.0 column and chemical suppression were used.

Samples for DOC analyses were also filtered and then analyzed on Shimadzu TOC analyzer TOC-5000 A (Shimadzu co., Kyoto, Japan) with the help of autosampler ASI-5000 A. The DOC was determined indirectly as the difference between dissolved total carbon (DTC) and dissolved inorganic carbon (DIC) (ISO 8245 1999).

The soil was air-dried and dry-sieved through 2-mm sieve (ISO 10390 2005, SIST ISO 11465 1993, ISO 11464 2006). Total carbon and total nitrogen (ISO 13878 1998) were analyzed with a CNS elemental analyzer LECO-CNS 2000 (LECO Corporation, Michigan, USA). In case of higher pH values, the inorganic carbon was determined as carbonate with Eijkelkamp (Eijkelkamp Royal, Giesbeek, The Netherlands) Scheibler's calcimeter and subtracted from the value of the total carbon (ISO 10693 1995).

The particle size distribution was determined by wet sieving through 0.063-mm sieve (sand) and pipetting at different times (coarse silt, fine silt, and clay).

The $\delta^{13}C_{DIC}$ was measured using an Isoprime 100 mass spectrometer, coupled with the Multiflow preparation module (Elementar, Manchester, UK). To prepare the sample, 100–200 µl of 100% phosphoric acid was added to a septum tube, which was then purged with pure He. Following this, 1 ml of the water sample was injected into the tube, and CO_2 was extracted and directly measured from the headspace. To ensure accuracy and normalize the $\delta^{13}C_{DIC}$ measurements, a standard solution of Na_2CO_3 (Carlo Erba) with a known $\delta^{13}C_{DIC}$ value of –10.8‰ ±0.2‰ was used, as described in Kanduč et al. (2007a, 2008).

The stable isotope ratios of carbon and nitrogen in particulate organic carbon ($\delta^{13}C_{POC}$ and $\delta^{15}N$) were measured using an Europa Scientific 20–20 continuous flow isotope ratio mass spectrometer (IRMS) with an ANCA-SL preparation module at the Jožef Stefan Institute. Following collection, three liter water samples was filtered through Whatman GF/F glass fiber filters (0.7 µm). The filters were treated with 1 M HCl to eliminate any carbonate material (if present), then dried at 60 °C, and stored until analysis. For carbon isotope analysis ($\delta^{13}C_{POC}$), approximately 1 mg of particulate organic matter (POM) was scraped from the filter and placed in a tin capsule. For nitrogen isotope analysis ($\delta^{15}N$), approximately 10 mg of POM was scraped from the filter without acid treatment. The isotopic composition of both carbon and nitrogen was determined following combustion of the capsules in a high-temperature furnace (1000 °C). The resulting gases were reduced in a copper tube at 600 °C. These gases were then separated via chromatography and ionized. NBS 22 (oil) and IAEA N-1 (ammonium sulfate) reference materials were used to calibrate the analytical results relative to the VPDB and AIR standards. The same sample preparation method used for the isotopic analysis of suspended particulate matter ($\delta^{13}C$ and $\delta^{15}N$) was also applied to sediment samples from soil profiles (with acid treatment for $\delta^{13}C$ analysis) and plant samples (with no acid treatment for both $\delta^{13}C$ and $\delta^{15}N$ analysis). All stable isotope results for carbon and nitrogen are expressed in the conventional delta (δ) notation, representing the per mil (%) deviation from the VPDB and AIR reference standards. Precision was ±0.2‰ for $\delta^{13}C_{DIC}$, $\delta^{13}C_{POC}$, $\delta^{13}C_{sediment}$, $\delta^{13}C_{plant}$ and ±0.3‰ for $\delta^{15}N_{sediment}$ and $\delta^{15}N_{plant}$.

2.3 Evasion Flux

The release of CO_2 from the Oplotnica River into the atmosphere, denoted as [DIC]ex, can be calculated using the thin-film diffusive gas exchange model (Broecker 1974):

$$[\mathrm{DIC}]_{ex} = {}^{D}/_{z} \times \left([\mathrm{CO_2}]_{eq} - [\mathrm{CO_2}] \right) \tag{2}$$

In this equation, D represents the diffusion coefficient of CO_2 in water, with values of 1.26 10^{-5} cm^2/s at 10 °C and 1.67 · 10^{-5} cm^2/s at 20 °C (Jähne et al. 1987). The variable [z] corresponds to the empirical thickness of the water surface layer [cm]. The terms $[CO_2]_{eq}$ and $[CO_2]$ indicate concentrations of dissolved CO_2 at equilibrium with the atmosphere and the sampled water [mol·cm^{-3}], respectively. The boundary layer, [z], is a thin film located at the interface between air and water, which varies depending on wind speed (Broecker et al. 1978) and water turbulence (Holley 1977). As a result, D/z represents thin gas transfer velocity, reflecting the height of the water column that equilibrates with atmospheric CO_2 over time. Based on an average wind speed of 4 m/s during all sampling seasons in the Oplotnica watershed (https://www.windfinder.com/forecast/oplotnica_oplotnica_slovenia), D/z was estimated at 8 cm/h under low turbulence conditions and 28 cm/h under moderate turbulence conditions. Data of T and pCO_2 for calculation of evasion flux are taken from the Oplotnica River.

2.4 Calculation of the Sources of Inorganic Dissolved Carbon Within the River System

$$\delta^{13}C_{DIC} = \delta^{13}C_{POC}x + (1 - x)\delta^{13}C_{atm} \tag{3}$$

x–share of degradation of organic matter.

(1-x)–share of equilibration with atmospheric CO_2.

where,

$\delta^{13}C_{DIC}$—isotopic composition of dissolved inorganic carbon.

$\delta^{13}C_{POC}$—isotopic composition of particulate organic carbon.

$\delta^{13}C_{atm}$—isotopic composition of atmospheric carbon in CO_2.

2.5 Calculation of the Sources of Particulate Organic Matter Within the River System

$$\delta^{13}C_{POC} = \delta^{13}C_{plant}x + (1 - x)\delta^{13}C_{soil} \tag{4}$$

where

$\delta^{13}C_{POC}$—isotopic composition of carbon in particulate organic carbon in the river.

$\delta^{13}C_{plant}$—isotopic composition of carbon in plant material (average $\delta^{13}C_{plant}$ is −30.4 ‰).

$\delta^{13}C_{soil}$—isotopic composition of carbon in soil material from sampling locations Tratice I, II, III (average $\delta^{13}C_{soil}$ is −26.0 ‰)

2.6 Thermodynamic Modeling

Thermodynamic computations were employed to evaluate the chemical speciation within the water system, including the partial pressures of CO_2 (pCO_2) and the saturation states of minerals. Inputs to the PHREEQC speciation program (Parkhurst and Appelo 1999) included pH, ion concentrations (Ca^{2+}, Mg^{2+}, Na^+, K^+), total alkalinity, and water temperature (only at the downstream location—1). The lack of data on Al and Si in the water system prevented the calculation of silicate mineral precipitation.

2.7 Statistical data Processing and Visualization

Pearson correlation analysis was conducted using Statistica 12.0 software, while plot visualization was performed using Excel version 2016.

2.8 Microscopy of Characteristic Rocks From a Catchment

The polished thin sections of the Pohorje rock were examined with a Nikon Eclipse E600 POL optical microscope (Department of Geology, University of Ljubljana). The samples were examined in transmitted parallel-polarized light at 100–1000 ×magnification and photo documented with the integrated Nikon DS-Fi1 camera and the NIS-Elements Basic Research program.

2.9 Presentation of Data in GIS Environment

Software ESRI ArcMap 10.5.1 was used for map production, with layers of the Basic Geological Map of Yugoslavia in scale 1:100,000, sheet L33-55 Slovenj Gradec (Mioč and Žnidarčič 1977). This information layer also defined the coordinate system of the map, the projected D48/GK Slovenian system (EPSG code 3912). Courses of rivers and creeks were obtained from the former EWNET-SI portal (http://ksh.fgg.uni-lj.si/ewnsi/enwnsi-eng.htm). Locations of sampling were determined in the field with GNSS receivers, and coordinates were transformed from WGS84 global system to the mentioned local projected system. For the background layer, we used a high-resolution (1 ×1 m) raster digital elevation model (DEM) obtained by laser (lidar) scanning in the period 2014–2015. Details about the scanning missions are available in the technical reports for the scanned areas on the official lidar data homepage: http://gis.arso.gov.si/evode/profile.aspx?id=atlas_voda_Lidar@Arso&culture=en-US.

3 Results

Basic characteristics of sampling sites, including physical and chemical properties during the period from 2012 to 2014 of surface waters in the Oplotnica River's catchment, are presented in Table 1. According to WRB (World reference base for soil resources), distric cambisoils are characteristics for Javorski and Lukanjski creeks downstream, while histosols are characteristic for both upstream locations (Table 1). The highest water temperature, 10.4 °C, was measured at the Oplotnica River, while the lowest, 3.9 °C, was measured at Javorski Creek. Also, seasonal changes of water temperature were detected; it is higher in summer period, while it is lower in winter period (Fig. 3a). The pH of all samples ranged from 5.7 to 6.8 with the highest pH detected at Oplotnica River. Lower pH was detected at Javorski creek, while higher pH was detected at Lukanjski creek (Table 1, Fig. 3b). At all sampling locations, a higher pH was detected in the summer period. The lowest electrical conductivity (EC) values ranged from 24.2 to 25.8 µS/cm at Javorski Creek (sites 1 and 2) and from 33.3 to 38.9 µS/cm at Lukanja Creek (sites 1 and 2); the highest EC, 86.8 µS/cm, was measured at the Oplotnica River (Fig. 3c, Table 1).

Sampling locations with underlying geology are presented in Fig. 1. Discharge, water temperature, pH, electrical conductivity, water geochemistry data in [mM] of surface waters along with isotopic composition of dissolved inorganic carbon ($\delta^{13}C_{DIC}$), particulate organic carbon ($\delta^{13}C_{POC}$) and isotopic composition of nitrogen ($\delta^{15}N$) along with thermodynamic modeling ($SI_{calcite}$ and $SI_{dolomite}$) are presented in Tables SM1 and SM2. All geochemical and isotopic data from surface waters of the Oplotnica watershed (Javorski creek, Lukanjski creek and Oplotnica River), along with soil profiles and plant data at sampling locations Tratice I, II, and III, have been uploaded to a public data repository (Kanduč et al. 2024).

The dominant major cations in the water samples are Na^+ and Ca^{2+}; their concentrations range from 0.048 to 0.187 mM and from 0.037 to 0.451 mM, respectively (Table SM 1). Concentrations of Mg^{2+} range from 0.011 to 0.206 mM (Table SM 1). HCO_3^- is the dominant anion with concentrations ranging from 0.003 to 1.153 mM (Table SM 1). DOC concentrations range from 0.110 to 1.352 mM (Table SM 1). Other results of cations and anions measured are presented in Table SM 1. $\delta^{13}C_{DIC}$ values range from −26.1 to −1.4‰ (Table SM 2) and reveal different biogeochemical processes in the water system. In

Table 1 Characteristics of sampling sites, including physical and chemical properties (average values of water sampled in the period of September, October, January, May, August, November, April, and June) during the period from 2012 to 2014 of surface waters in the Oplotnica River catchment

Abbreviation on the map	Location name/type of sampling	Area [m^2]	Elevation [m]	LAT [°] (WGS84)	LONG [°] (WGS84)	SOIL UNIT (WRB* classification)	Q [m^3/s]	T [°C]	pH	EC [µS/cm]
JC1	Javorski Creek 1 downstream/water		1274	46.463579	15.387476	Distric cambisols	3.4	3.9	5.9	24.2
JC1 s	Javorski creek 1/Soil, three soil profiles: Tratice I, Tratice II, Tratice III		1293	46.463889	15.387065	Distric cambisols				
JC2	Javorski Creek 2 upstream/water	222,243	1292	46.465762	15.389352	Histosols	n.d	n.d	5.7	25.8
LC1	Lukanjski creek 1 downstream/water		1174	46.448947	15.399047	Distric cambisols	3.9	4.5	6.4	33.3
LC2	Lukanjski creek 2 upstream/water	209,116	1227	46.451070	15.401061	Histosols	n.d	n.d	6.4	38.9
OR	Oplotnica River, before entering village Oplotnica/water		415	46.397196	15.442676		1.2**	10.4	6.8	86.8

*WRB—World reference base for soil resources

**Average discharge (Q) at Perovec gauging station for year 2017

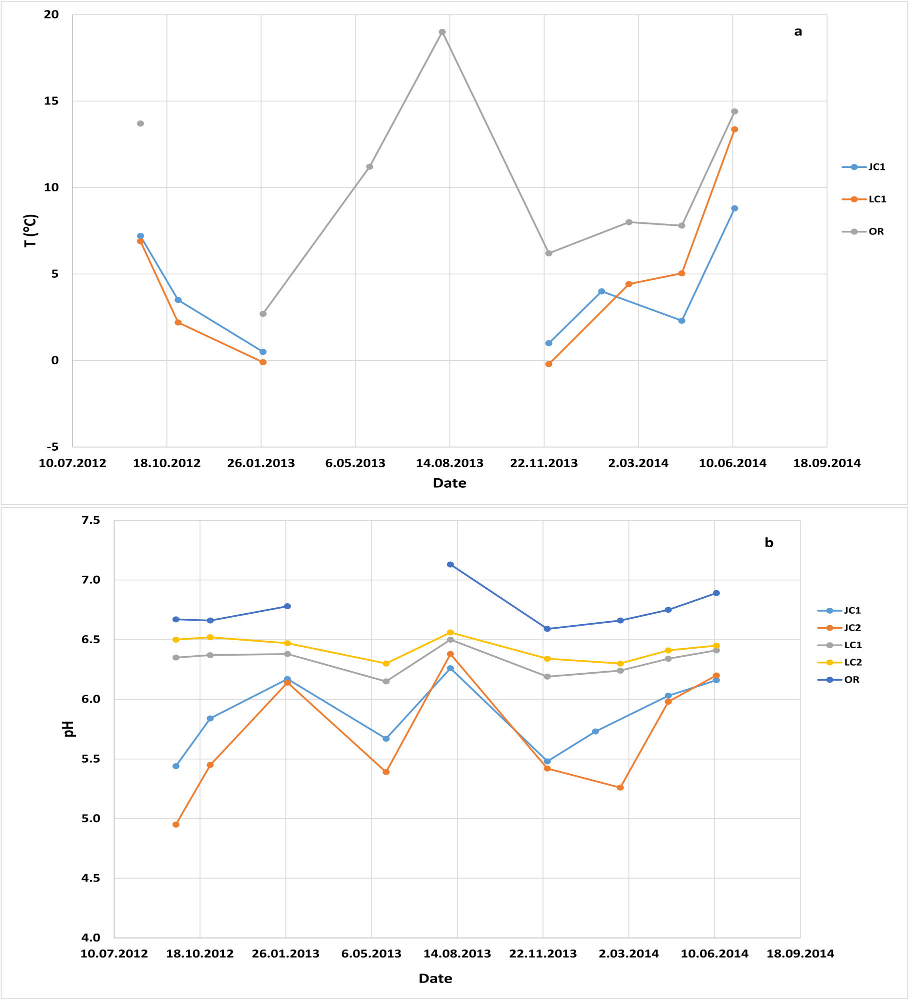

Fig. 3 Temporal changes of **a** water temperature **b** pH **c** electrical conductivity, JC1—Javorski Creek 1, JC2—Javorski Creek 2, LC1—Lukanjski Creek 1, LC2—Lukanjski Creek 2, OR—Oplotnica River

suspended matter, $\delta^{13}C_{POC}$ values range from − 28.2 to −22.3‰, while $\delta^{15}N$ values range from −2.2 to 2.6‰ (Table SM2). pCO_2 ranges from −3.4 to −2.3 bars and indicates 1.1 to 13.4 times over saturation. Saturation indices for calcite ($SI_{calcite}$) range from −6.1 to −1.9, while SI for dolomite ($SI_{dolomite}$) ranges from −12.7 to −4.2 (Table SM 2). Both minerals (calcite and dolomite) are undersaturated and should dissolve in water.

The characteristics of soil samples from Javorski Creek – JC1 s (Tratice I, Tratice II, Tratice III) are presented in Table 2 and Table SM 3, including sieve analyses. At all three locations, the carbon (C) concentrations range from 18.6 to 52.3% in the organic-rich layer and from 0.8 to 13.3% in the mineral soil layer. Nitrogen (N) concentrations range from 1.0 to 1.8% in the upper soil layer and from 0.05 to 0.07% in the lower layer. The C/N ratio ranges from 18.1 to 39.6 in the upper soil layer and from 16.5 to 21.5 in the lower layer (Table 2). The $\delta^{13}C$ values in the upper organic horizon range

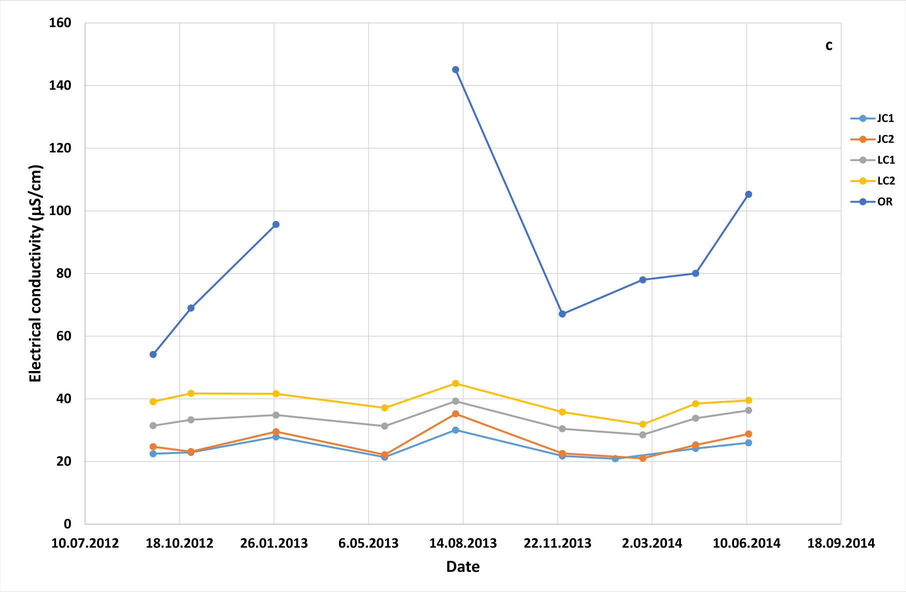

Fig. 3 (continued)

from −28.3 to −25.6‰, while in the mineral soil horizon they range from −26.0 to −24.9‰ (Table 2). The δ^{15}N values range from −4.9 to −1.5‰ in the upper horizon and from −4.0 to 5.4‰ in the lower mineral soil horizon (Table 2). Sand predominates over fine and coarse silt and clay in all analyzed samples in the mineral layers from 5 to 80 cm depth (Table SM 3). Leaves and needles of plants have an average δ^{13}C value of −30.4‰ and an average δ^{15}N value of −6.8‰ (Table SM 4).

4 Discussion

4.1 Temporal Changes of Water Geochemistry

The major solute composition of the Oplotnica River and its tributaries is dominated by $Na^+ > Ca^{2+} > Mg^{2+} > K^+$ and $HCO_3^- > SO_4^{2-} > Cl^- > NO_3^-$. Concentrations varied seasonally in relation to discharge, with lower concentrations observed in spring and autumn at lower discharge, and higher concentrations during the winter and summer sampling seasons (Fig. 4 a-i). The concentrations of cations (Na^+, Ca^{2+}, Mg^{2+}, K^+) and anions (HCO_3^-, SO_4^{2-}, Cl^-, NO_3^-) were highest in the Oplotnica River across all sampling seasons and lowest in Javorski Creek 1 (Fig. 4 a-i).

Dissolved organic carbon (DOC) concentrations reached up to 1.83 mM during both sampling seasons in Idrijca tributaries located in carbonate/clastic environments (Kanduč et al. 2008). However, much lower DOC concentrations, up to 1.3 mM (Fig. 4i), were observed in this study's silicate-dominated setting. The export of DOC from land to aquatic ecosystems and the oceans is a significant vector of carbon transport across continents and

Table 2 Pedological survey of horizons with C, N concentrations, δ^{13}C and δ^{15}N at Javorski creek 1 (JC1 s)

Horizon	Depth [cm]	$C_{org.}$ [%]	N[%]	$C_{org.}$/N	δ^{13}C[‰]	δ^{15}N[‰s]
Ol (litter layer)	0.86	52.32	1.32	39.62	− 28.3	− 4.6
Of (Fermentation layer)	0.79	46.10	1.72	26.83	− 27.6	− 4.2
Oh (Humus layer)	0.38	20.84	1.15	18.10	− 25.8	− 1.9
M5 (Mineral soil layer at 5 cm depth)	− 2.5	10.91	0.66	16.53	− 26.0	− 4.0
M10 (Mineral soil layer at 10 cm depth)	− 10	7.58	0.42	18.14	− 25.7	2.8
M20 (Mineral soil layer at 20 cm depth)	− 15	5.90	0.31	19.06	− 26.0	3.6
M40 (Mineral soil layer at 40 cm depth)	− 30	4.00	0.19	21.52	− 26.0	5.4
M60 (Mineral soil layer at 60 cm depth)	− 50	1.88	0.09	20.38	− 25.2	4.1
M80 (Mineral soil layer at 80 cm depth)	− 70	0.82	0.05	18.06	− 25.0	4.0
Ol (Litter layer)	5	51.52	1.83	28.21	− 27.4	− 3.4
Of (Fermentation layer)	1.67	33.91	1.64	20.66	− 26.0	− 4.0
Oh (Humus layer)	0.33	18.57	1.00	18.53	− 26.0	− 1.5
M5 (Mineral soil layer at 5 cm depth)	− 2.5	9.97	0.60	16.58	− 26.0	0.5
M10 (Mineral soil layer at 10 cm depth)	− 7.5	6.90	0.42	16.46	− 25.8	3.3
M20 (Mineral soil layer at 20 cm depth)	− 15	5.56	0.32	17.37	− 25.8	4.6
M40 (Mineral soil layer at 40 cm depth)	− 30	3.52	0.18	19.24	− 25.7	5.2
M60 (Mineral soil layer at 60 cm depth)	− 50	1.69	0.09	17.92	− 24.9	3.9
M80 (Mineral soil layer at 80 cm depth)	− 70	1.35	0.07	18.49	− 25.3	5.2
Ol (Litter layer)	1.05	51.27	1.41	36.27	− 28.0	− 4.9
Of (Fermentation layer)	0.73	44.08	1.80	24.47	− 27.2	− 4.4
Oh (Humus layer)	0.33	25.53	1.37	18.60	− 25.6	− 2.5
M5 (Mineral soil layer at 5 cm depth)	− 2.5	13.34	0.77	17.25	− 25.5	0.0
M10 (Mineral soil layer at 10 cm depth)	− 7.5	7.98	0.45	17.80	− 25.7	2.1
M20 (Mineral soil layer at 20 cm depth)	− 15	6.57	0.35	18.76	− 25.7	3.6
M40 (Mineral soil layer at 40 cm depth)	− 30	3.43	0.17	20.40	− 25.5	4.7
M60 (Mineral soil layer at 60 cm depth)	− 50	2.85	0.14	20.22	− 25.4	3.8
M80 (Mineral soil layer at 80 cm depth)	− 70	1.47	0.08	18.16	− 25.5	5.1

The reference zero depth (Table 2) in the soil profile is defined at the upper layer of the M5 mineral layer

local landscapes (Roulet and Moore 2006). The DOC values observed in this silicate catchment are typical of unpolluted rivers (Tao 1998).

Furthermore, we performed Pearson statistical correlation analysis between the variables: water temperature (T), pH, conductivity, Na^+, K^+, Ca^{2+}, Mg^{2+}, NO_3^-, SO_4^{2-}, Cl^-, dissolved organic carbon (DOC), and total alkalinity. Significant positive correlations ($p < 0.05$) were observed between various parameters. Conductivity showed strong correlations with total alkalinity ($r = 0.99$), Cl^- ($r = 0.86$), Mg^{2+} ($r = 0.99$), Ca^{2+} ($r = 0.99$), K^+ ($r = 0.97$), and Na^+ ($r = 0.93$). Additionally, Na^+ correlated with SO_4^{2-} ($r = 0.92$) and Ca^{2+} ($r = 0.91$). K^+ correlated with Mg^{2+} ($r = 0.98$) and Ca^{2+} ($r = 0.98$). Strong correlations were also found between SO_4^{2-} and NO_3^- ($r = 0.93$), total alkalinity and K^+ ($r = 0.98$), Ca^{2+} and total alkalinity ($r = 0.99$), and Mg^{2+} and total alkalinity ($r = 0.99$). Weak but significant negative correlations ($p < 0.05$) were found between NO_3^- and DOC ($r = -0.50$) and SO_4^{2-} and DOC ($r = -0.63$). These high statistical correlations are attributed to natural geogenic factors, as no significant industrial activity is present in the catchment area (Fig. 1).

Fig. 4 Temporal changes of major cations: **a** Na^+, **b** Ca^{2+}, **c** Mg^{2+}, **d** K^+, **e** HCO_3^-, **f** SO_4^{2-}, **g** Cl^-, **h** NO_3^- **i** DOC in Javorski (JC) and Lukanjski (LC) Creeks and Oplotnica River (OR)

4.2 Origin of Ca^{2+} and Mg^{2+} in Water System

Dissolved Ca^{2+} and Mg^{2+} in the silicate catchment area are largely supplied by the weathering of mafic minerals and feldspars (albite, anorthite), with significant contributions from silicate weathering. This is indicated by the relatively low HCO_3^- concentrations, which

Fig. 4 (continued)

are below 1.2 mM (Fig. 5a). Figure 5a shows the relationship between Ca^{2+} + Mg^{2+} and total alkalinity. Most samples in this study exhibit a 1:1 molar ratio of HCO_3^- (measured as total alkalinity) to Ca^{2+} + Mg^{2+}, following the weathering reactions of albite, anorthite, orthoclase, and chlorite (Kanduč et al. 2023). In watersheds primarily composed of carbonates, such as the River Sava watershed in Slovenia, the Ca^{2+} + Mg^{2+} ratio ranges from 0.6 to 1.6 mM, while HCO_3^- concentrations range from 1.2 to 3.2 mM (Szramek et al. 2007).

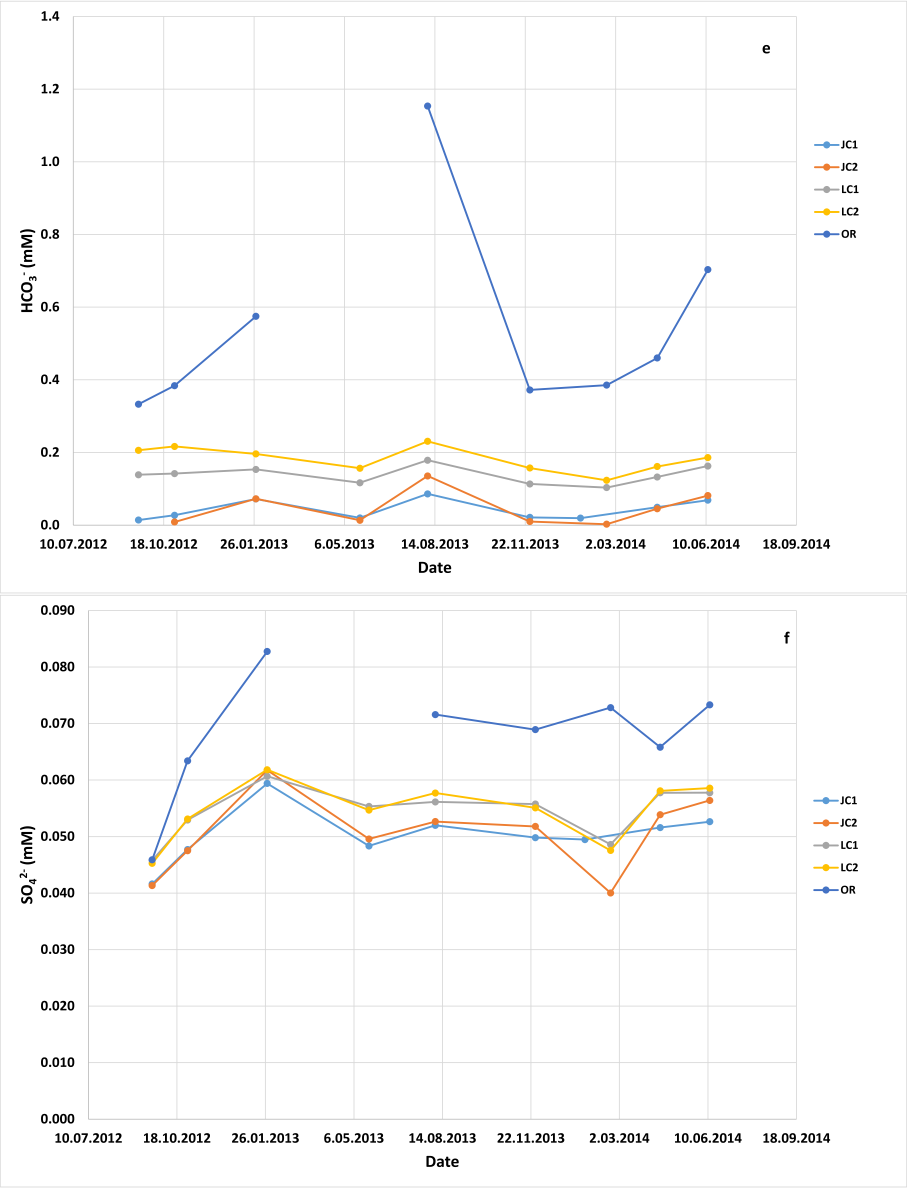

Fig. 4 (continued)

A similar ratio (Ca^{2+} + Mg^{2+} from 0.87 to 2.66 mM and total alkalinity from 1.6 to 5.6 mM) was found for the Kamniška Bistrica River (Kanduč et al. 2013). In comparison, the Ca^{2+} + Mg^{2+} ratio in the silicate catchment studied here ranges from 0.05 to 0.7 mM, with HCO_3^- concentrations varying between 0.003 and 1.153 mM (Table SM1), indicating much lower ratios and concentrations. The water samples in this study deviate from the 1:2 line (Fig. 1a), which is typical for carbonate weathering. In general, HCO_3^- concentrations

Fig. 4 (continued)

in silicate-dominated watersheds are low (around 1 mM) compared to carbonate watersheds (up to 6 mM) (Kanduč et al. 2008, 2013).

Figure 5b illustrates the relationship between Mg^{2+} and Ca^{2+}, thereby determining the relative contributions of Mg^{2+} and Ca^{2+} in the Oplotnica watershed. Previous studies have shown that Slovenian streams exhibit a wide range of Mg^{2+}/Ca^{2+} ratios, reflecting variations in the relative contributions of calcite and dolomite across different tributaries,

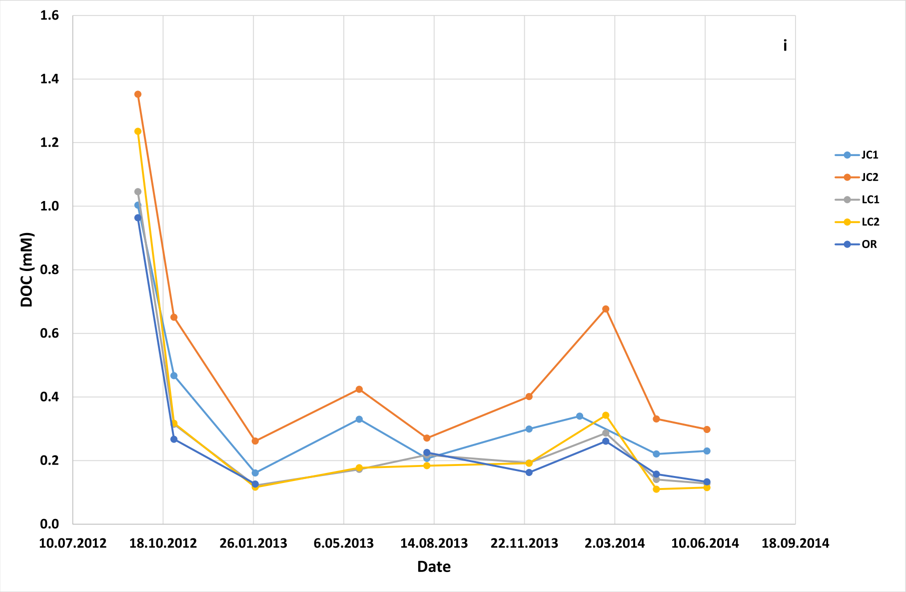

Fig. 4 (continued)

with values ranging from 0.2 to nearly 0.8 (Szramek et al. 2007). In the River Oplotnica, a lower range of Mg^{2+}/Ca^{2+} ratios (from 0.2 to 0.5), originating from mafic minerals and feldspars, has been observed. However, it is important to emphasize that Ca^{2+} dominates over Mg^{2+} (Fig. 5b). A Mg^{2+}/Ca^{2+} ratio around 0.33, which is typical for the weathering of magnesium-containing calcite in carbonate watersheds, has also been observed in water samples from the silicate-dominated Oplotnica catchment (Fig. 5b).

The calcite saturation index was generally well below equilibrium ($SI_{calcite} = 0$) (Fig. 6c), indicating that calcite and dolomite were undersaturated and likely to dissolve (Fig. 6c). Similar observations were found in the Svratka watershed (Kanduč et al. 2023), but opposite in carbonate—bearing environments, where $SI_{calcite}$ and $SI_{dolomite}$ are well above equilibrium and more likely to precipitate (Kanduč et al. 2013, 2023).

4.3 Carbon Sequestration and Movement in river Watershed

Carbon cycling in river systems involves both organic and inorganic components (Mayorga et al. 2005), although in this study there was no clear pattern between total alkalinity and DOC (dissolved organic carbon) (Fig. 6a). Calculated CO_2 partial pressures (pCO_2) varied from 436 to 5370 ppm in all sampling locations (Fig. 6b). Normal atmospheric pressure is around 400 ppm according to Lan et al. (2024). All sampling locations in the catchment are above equilibrium with atmospheric CO_2, except one sampling location at Javorski creek. These higher partial pressures in all sampling seasons are probably related to low pH (from 4.95 to 7.13) throughout the investigated period. The theoretical CO_2 diffusive evasion rates at all locations and across all period, according to Eq. (2), ranged from $1.19{\cdot}10^{-6}$ to $3.4{\cdot}10^{-4}$ mol/cm$^2{\cdot}$h (under low turbulence conditions) and $4.18{\cdot}10^{-6}$ to $1.2{\cdot}10^{-3}$ mol/cm$^2{\cdot}$h (under moderate to high turbulence conditions). Taking into consideration the river

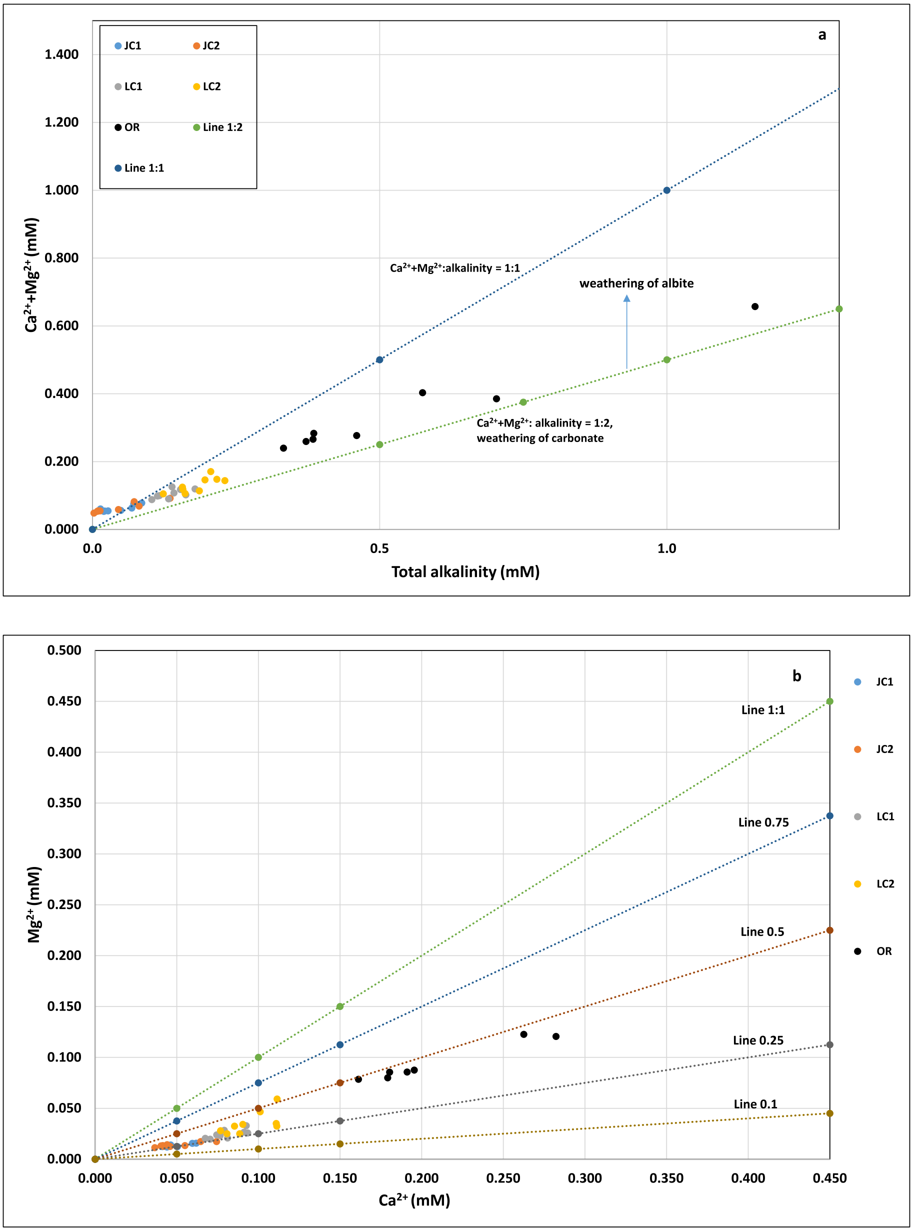

Fig. 5 **a** $Ca^{2+}+Mg^{2+}$ versus total alkalinity, **b** Mg^{2+} versus Ca^{2+}

surface area of 52 km^2 (Perovec gauging station at the River Oplotnica), the estimated total diffusive loss of inorganic carbon varies seasonally under low turbulence conditions, ranging from $5.7 \cdot 10^3$ mol/day (September 2012) to $1.67 \cdot 10^7$ mol/day (May 2013) at the Perovec location. Under high turbulence conditions, the evasion fluxes range from $2.07 \cdot 10^5$

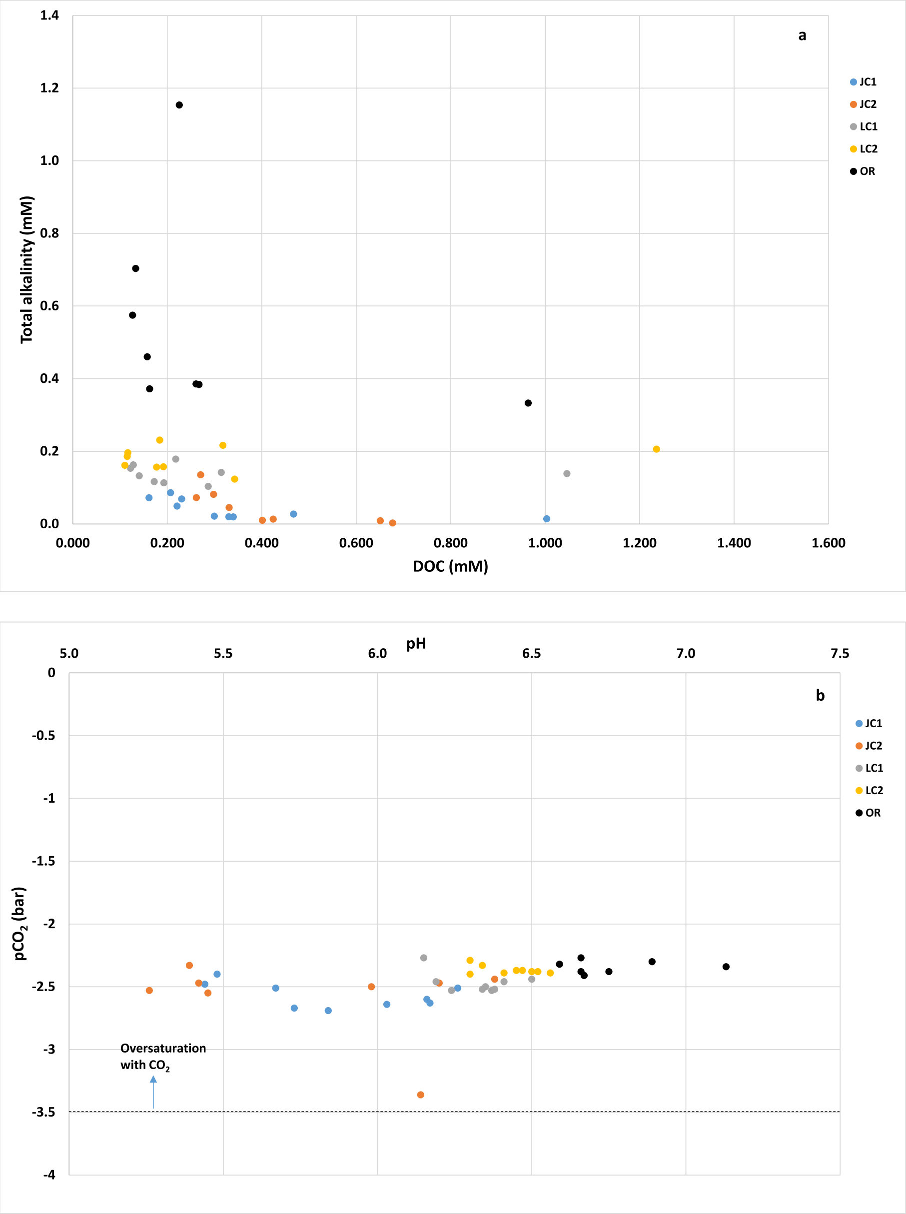

Fig. 6 **a** Total alkalinity versus DOC, **b** pCO$_2$ versus pH, **c** SI$_{calcite}$ versus SI$_{dolomite}$, **d** δ^{13}C$_{DIC}$ versus total alkalinity, **e** δ^{13}C$_{POC}$ versus δ^{13}C$_{DIC}$

to 2.87·10^7 mol/day. At the VRA location (Svratka River), the estimated total diffusive loss of inorganic carbon under low turbulence conditions is 2.9·10^4 mol C/day in January 2012, 5.9·10^5 mol C/day in June 2012, 2.2·10^6 mol C/day in December 2013, and 8.0·10^5 mol C/day in July 2014 (Kanduč et al. 2023). Under moderate turbulence conditions, the total diffusive loss of inorganic carbon varies seasonally, ranging from 1.0·10^5 to 7.8·10^6 mol C/

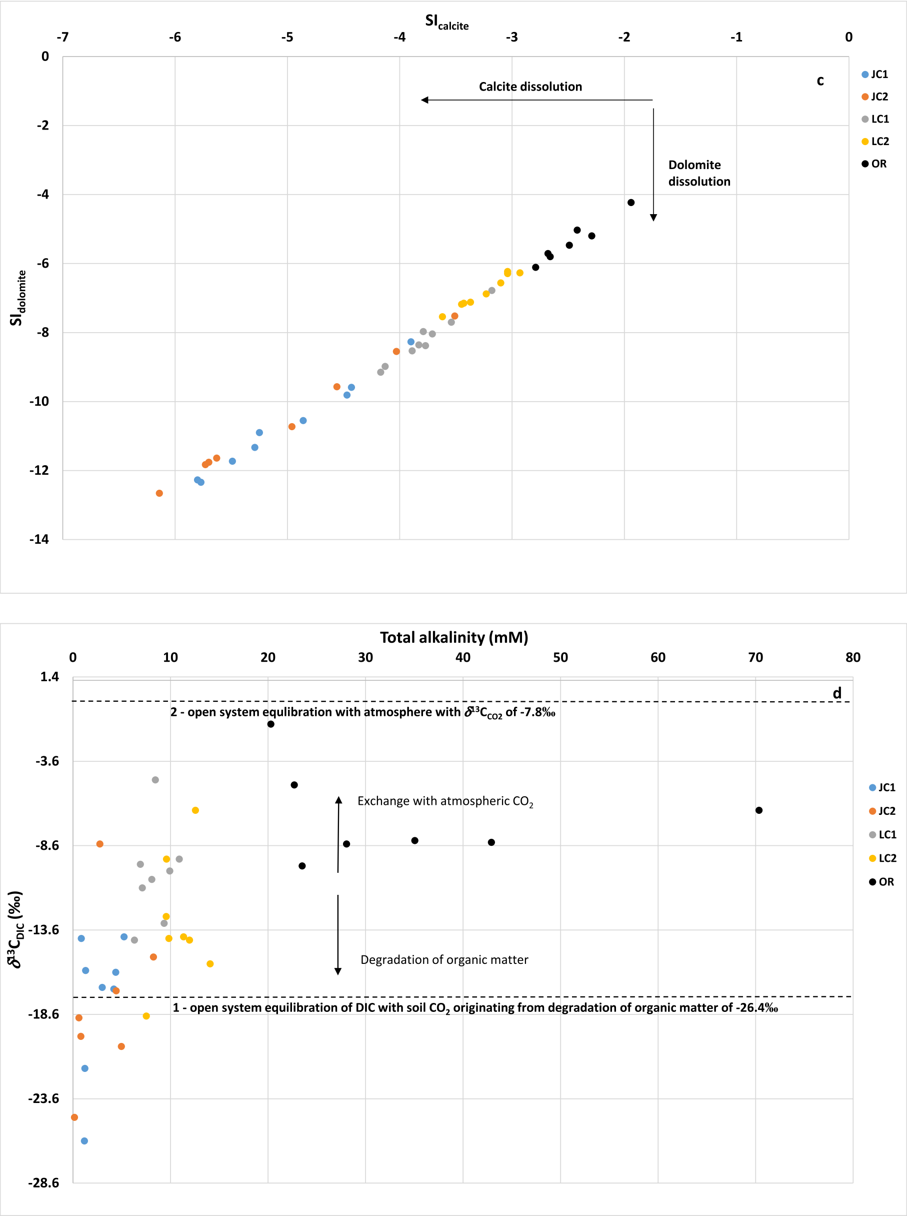

Fig. 6 (continued)

day. Compared to the Svratka River, higher evasion fluxes were observed for the Oplotnica River. The CO_2 evasion flux is consistently positive along the creeks and river flow throughout the investigated period (Fig. 6b), which is not the case for the Svratka River.

In river systems, several processes influence $\delta^{13}C_{DIC}$. Direct oxidation of organic matter decreases $\delta^{13}C_{DIC}$, while photosynthesis increases it (Mook and Tan 1991). The dissolution

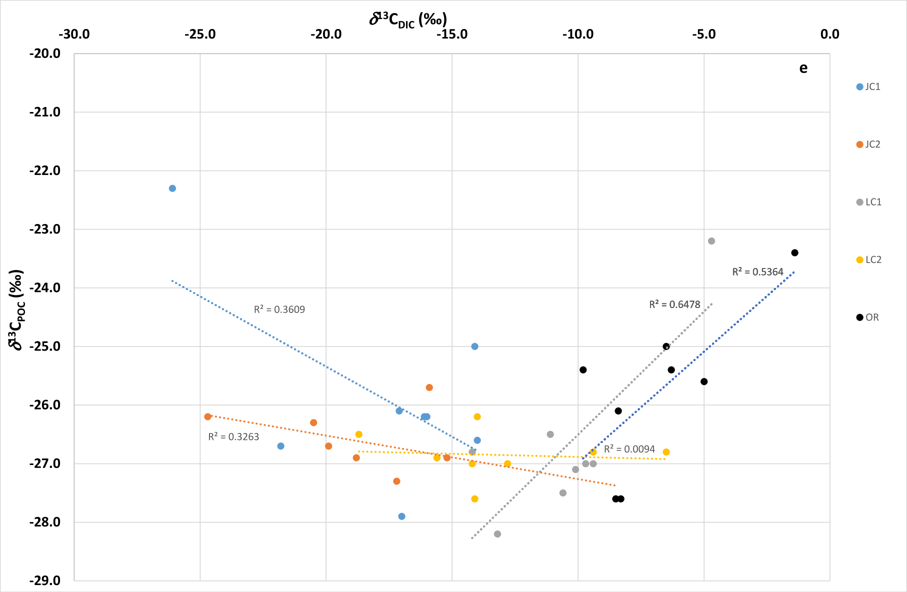

Fig. 6 (continued)

of carbonate minerals in streams increases $\delta^{13}C_{DIC}$, whereas precipitation of carbonates lowers it due to equilibrium fractionation between calcite and DIC, which is approximately 2 ‰ (Aucour et al. 1999). Additionally, CO_2 exchange between the river and the atmosphere affects $\delta^{13}C_{DIC}$ values, pushing them toward equilibrium with atmospheric CO_2, resulting in a $\delta^{13}C_{DIC}$ value of about 1 ‰ (Mook 1970; Yang et al. 1996).

The average $\delta^{13}C_{POC}$ value of −26.4 ‰ from all measured locations (rivers and tributaries) was used to calculate isotope fractionation lines (Fig. 6d). Open-system equilibration of DIC with CO_2 from POC enriches DIC in $\delta^{13}C$ by about 9 ‰, corresponding to a value of −17.4 ‰ (Fig. 6d). DIC in equilibrium with the atmosphere should have a $\delta^{13}C_{DIC}$ of approximately +1.2 ‰. Both biogeochemical processes—organic matter degradation and equilibration with the atmosphere—influence the $\delta^{13}C_{DIC}$ values in water samples from the Oplotnica catchment. A simple mass balance calculation was performed to determine seasonal contributions during the investigated period. Both contributing sources, atmospheric CO_2 (+ 1.2 ‰) and organic matter degradation (− 26.1 ‰), were included in the mass balance calculation according to Eq. 3. The results of the mass balance calculations are as follows: $\delta^{13}C_{POC}$ contributes between 44.4% and 100%, while $\delta^{13}C_{atm}$ contributes between 0 and 95.6%. Interestingly, some samples (with low $\delta^{13}C_{DIC}$) deviate from the fractionation line (1), indicating nonequilibrium between DIC and soil CO_2 (Fig. 6d).

Carbon dissolution and its effect on $\delta^{13}C_{DIC}$ values were omitted in the Oplotnica catchment since the catchment is mostly composed of feldspars and siliciclastic rocks. Higher $\delta^{13}C_{DIC}$ values were observed in the Oplotnica River, while lower values were found in both investigated creeks (down to −26.1 ‰, Fig. 6d), indicating that at upstream locations of Javorski creek, the degradation of organic matter is the most important biogeochemical processes. We observe no clear pattern between $\delta^{13}C_{DIC}$ and $\delta^{13}C_{POC}$ values (Fig. 6e).

The primary control on carbonate weathering intensity is runoff (Amiotte Suchet and Probst 1993). Carbonate weathering intensity normalized to drainage area quantifies the production of HCO_3^- from mineral weathering. The pH, temperature, and pCO_2 of a watershed determine the carbonate speciation, controlling the HCO_3^- carrying capacity. In Slovenian watersheds, total alkalinity comprises carbonate alkalinity (Kanduč et. al. 2007a), and therefore, total alkalinity is assumed as HCO_3^-, which is the main DIC species at the pH of 6.4 to 10.3 (Clark and Fritz 1997). The black lines on the provided plot (Fig. 7) represent contours of bicarbonate (HCO_3^-) concentration (mmol/L). These lines indicate constant bicarbonate concentration levels (from 1 to 5 mmol/L). Each line shows combinations of HCO_3^- weathering intensity (y-axis) and specific runoff (x-axis) that correspond to a given bicarbonate concentration. Points on the same line have equal bicarbonate concentration but vary in weathering intensity and runoff. Therefore, the black lines (Fig. 7) help illustrate the relationship between weathering intensity and runoff at specific constant bicarbonate concentrations, allowing easier comparison of the measured data points against these reference levels. Bicarbonate concentrations (represented by the black lines in Fig. 7) below or around 1 mmol/L are typical of silicate weathering, while concentrations above 3 mmol/L are typical of carbonate—bearing environments. Weathering capacity at Oplotnica River is 10.4 mol/km^2·s. Figure 7 compares carbonate weathering intensities as a function of specific runoff for the watershed, combining new data from this study with published official data for the river Sava (largest river in Slovenia) and data from Berner and Berner (1996) for world rivers and the Danube.

Additionally, we plotted data of total alkalinity for silicate Svratka River (Fig. 7, Kanduč et al. 2023) for comparison with carbonate/clastics bearing rivers. Global theoretical models of CO_2 consumption in carbonate watersheds show an alkalinity value around 3 mmol/1 determined from a best-fit line (Amiotte Suchet and Probst 1993). The climate and topographic relief in Slovenian watersheds importantly influence

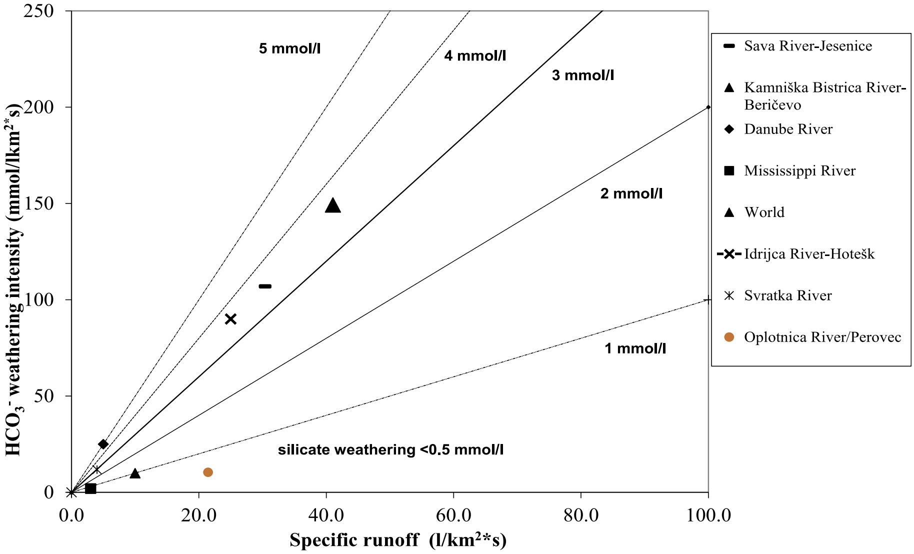

Fig. 7 HCO_3^- weathering intensity of Oplotnica River at Perovec compared to worldwide rivers

the carbonate weathering intensity and specific runoff. The watershed of the River Oplotnica is predominantly a silicate environment with weathering capacity of 10.4 mmol/(l·km^2·s). The world average value for carbonate weathering intensity is 7 mmol/(l·km^2 ·s), which is comparable with Oplotnica River at Perovec gauging location. From Fig. 7, it can be observed that carbonate rivers (e.g., Kamniška Bistrica, River Sava at Jesenice, Idrijca River) investigated in Slovenia have much higher carbonate weathering capacity than silicate rivers.

4.4 Origin of Suspended Matter in Oplotnica River System

Combining δ^{13}C and δ^{15}N values with C/N ratios can more accurately trace OM sources, making an integrated study of temporal and spatial variations in δ^{13}C, δ^{15}N, and C/N important for characterizing sources of organic matter in aquatic systems (Li et al. 2020; Thomson et al. 2018). In our study, C/N ratio was measured with associated parameters δ^{13}C and δ^{15}N only in soil profiles at sampling location JC1 s (Fig. 1, Table 1). Distribution ranges of δ^{13}C, δ^{15}N, C/N ratios of different end-members (soil, atmospheric deposition, C4 plants, C3 plants, macrophytes, phytoplankton) are presented in Table 3.

The upper horizons (Oh, Of, and Ol layers) contain high $C_{org.}$/N ratios, ranging from 18.1 to 39.6%, which is characteristic of C3 plants (Table 3, Fig. 8a). The lower mineral layers have C/N ratios ranging from 16.4 to 21.5%, indicating degraded C3 plant debris (Table 3). The average soil value of δ^{13}C, which is − 26.0‰ across all three sampling locations (Tratice I, II, III), falls within the range characteristic of soil values (Table 3; Kendall et al. 2001; Lu et al. 2012). The average δ^{15}N in soil for Tratice is 1.0‰ (Table 2), which is 1‰ more negative than the values presented in Table 3 (Ren et al. 2024 and references therein).

Soils are enriched in ^{13}C and ^{15}N, likely due to organic matter degradation and microbial activity, which increases δ^{13}C and δ^{15}N values in soils (Staddon 2004). Naturally isotopically depleted organic materials may be utilized by microorganisms, while the remaining organic matter becomes enriched in the heavier ^{13}C and ^{15}N isotopes (Figs. 8b, c).

Temporal changes and the origins of carbon and nitrogen are presented in Figs. 9a and b. The highest $\delta^{13}C_{POC}$ values are observed during the winter period at Javorski Creek 1 and Lukanjski Creek, likely due to an influx of microbially derived material. Seasonal variations are observed between sampling locations and are associated with leaching from terrestrial sources (Figs. 8b, c). Lower $\delta^{13}C_{POC}$ values indicate organic material with a lower organic composition, while higher values reflect microbially degraded material (Fig. 8c).

In the Oplotnica River's catchment and its rivers and creeks, the average $\delta^{13}C_{POC}$ is −26.4‰, similar to that in the Idrijca River soil profiles (average of −26.6‰), indicating that POC mainly originates from organic matter decomposition rather than plants, macrophytes, or phytoplankton, which typically exhibit more negative δ^{13}C values, reaching up to −42‰ (Table 3). Additionally, the δ^{15}N of particulate matter aligns with values characteristic of soils and atmospheric deposition (Table SM 2, Fig. 9b) (Kanduč et al. 2008). According to a simple mixing model, the proportions of soil and plant litter in particulate organic carbon (POC) can be calculated using Eq. 4. Mass balance calculations reveal that more than 93.4% of POC in the river system is contributed by soil, with only a minor portion, up to 6.6%, derived from plant material.

Table 3 Distribution ranges of $\delta^{13}C$, $\delta^{15}N$, C/N ratios of different end-members (Ren et al. 2024)

End-member	$\delta^{13}C$ (‰)	$\delta^{15}N$ (‰)	C/N	References
Soil	from −26 to (−21.18)	from 2 to 5	from 9 to 12.5	Kendall et al. 2001; Lu et al. 2012
Sewage	from −28.5 to (−23)	from 7 to 25	from 6.6 to 13	Guo et al. 2020
Atmospheric deposition	from −26 to (−23)	from −7 to 2	from 23 to 46	Guo et al. 2020
C4 plants	from −17 to (−9)	from 3 to 6	from 15 to 29	Guo et al. 2020, Lu et al. 2012
C3 plants	from −30 to (−23)	from −5 to 18	from 18 to 38	Guo et al. 2020, Lu et al. 2012
Macrophytes	from −28 to (−18)	from −15 to 20	from 10 to 30	Kendall et al. 2001; Tang and Zhang 2010
Phytoplankton	from −42 to (−24)	from −15 to 20	from 3 to 8	Tang and Zhang 2010; Yang et al. 2020

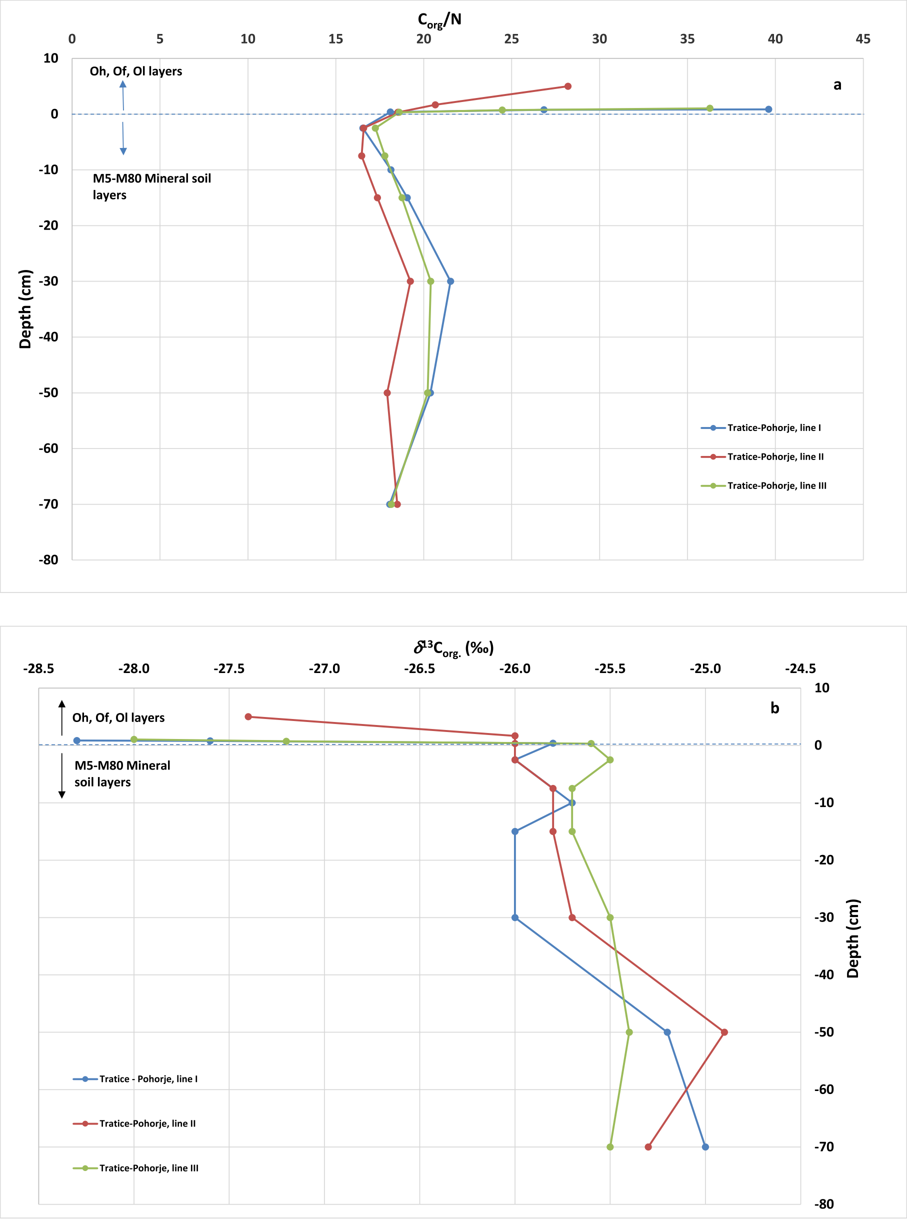

Fig. 8 Soil characterization at JC1 s sampling location Tratice, Pohorje: Tratice I, Tratice II, Tratice III: **a** C_{org}/N versus depth, **b** $\delta^{13}C_{org.}$ versus depth **c** $\delta^{15}N$ versus depth

5 Conclusion

During the investigated period 2012–2014, the major solute composition of the Oplotnica River silicate catchment is dominated by HCO_3^-, Ca^{2+}, Na^+, Mg^{2+}, and Cl^-,

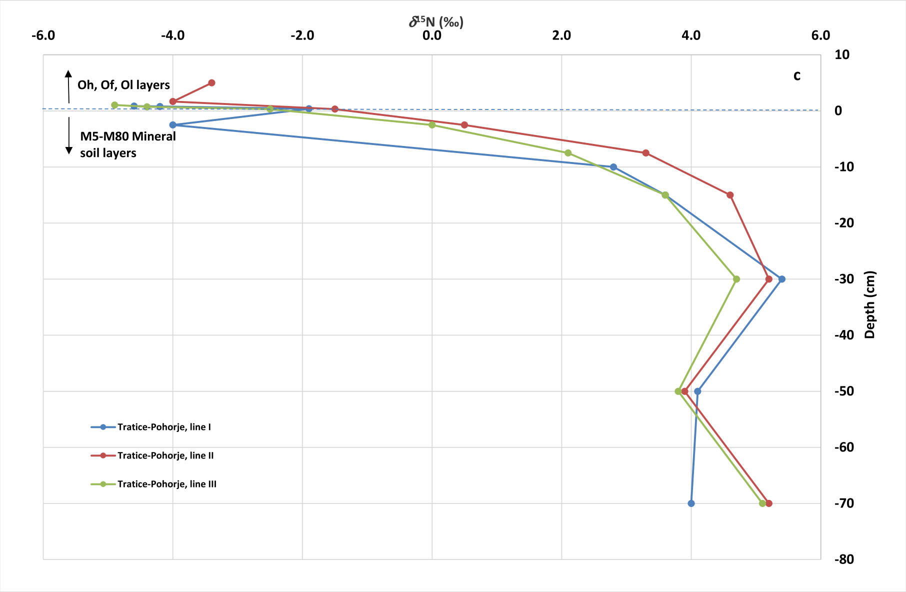

Fig. 8 (continued)

while in the creeks, the dominant ions are HCO_3^-, Na^+, Ca^{2+}, Mg^{2+}, NO_3^-, Cl^-, K^+, and SO_4^{2-}. The bicarbonate weathering intensity of the Oplotnica River is 10.4 mmol/(l·km^2·s), which is typical for silicate rivers worldwide.

$\delta^{13}C_{DIC}$ values range from −26.1 to −1.4‰, indicating: (1) open system equilibration with the atmosphere, and (2) soil CO_2 originating from the degradation of organic matter with $\delta^{13}C_{POC}$ of −26.4‰. Mass balance calculations for carbon isotopes revealed that, on average, the contribution of $\delta^{13}C_{POC}$ is 47.2%, while $\delta^{13}C$ atmospheric is 52.8%. $\delta^{13}C_{POC}$ in the river system indicate that POC is mainly originated from soil material (up to 93.4%). Based on thermodynamic modeling, the Oplotnica River and its tributaries represent a source of CO_2 to the atmosphere during the investigated period from 2012 to 2014. Compared to other investigated Slovenian rivers (the Idrijca River and the Sava River) and the Svratka River, the Oplotnica River has a higher CO_2 evasion flux.

In the Oplotnica River, the highest $\delta^{13}C_{POC}$ values are observed during the summer period, indicating increased organic degradation. In contrast, however lower $\delta^{13}C_{POC}$ values are observed in the winter, spring, and autumn period, likely due to increased surface leaching. Lower $\delta^{13}C$ and $\delta^{15}N$ values in sediments are detected in the upper horizons of JC1 s (ranging from −28.3 to −25.0 ‰ for carbon and from −4.9 to −1.5 ‰ for nitrogen), whereas higher $\delta^{13}C$ and $\delta^{15}N$ values were detected in the lower horizons of JC1 s (ranging from −26.0 to −24.9 ‰ for carbon and from −4.0 to 5.4 ‰ for nitrogen). These values fall within the same range as those found in particulate matter in river water (average $\delta^{13}C$ value of −26.4 ‰ and $\delta^{15}N$ value of 0.7 ‰). The weathering of metamorphic minerals such as feldspar, muscovite, biotite, calcite, dolomite, and quartz within the watershed contributes to the total alkalinity and solute composition of river waters.

Major ion chemistry and stable isotopes have proved to be useful tracers of biogeochemical processes in river systems. $\delta^{13}C$ and $\delta^{15}N$ in sediments, rivers, and particulate matter are additional tracers of the sources of carbon and nitrogen in catchment areas.

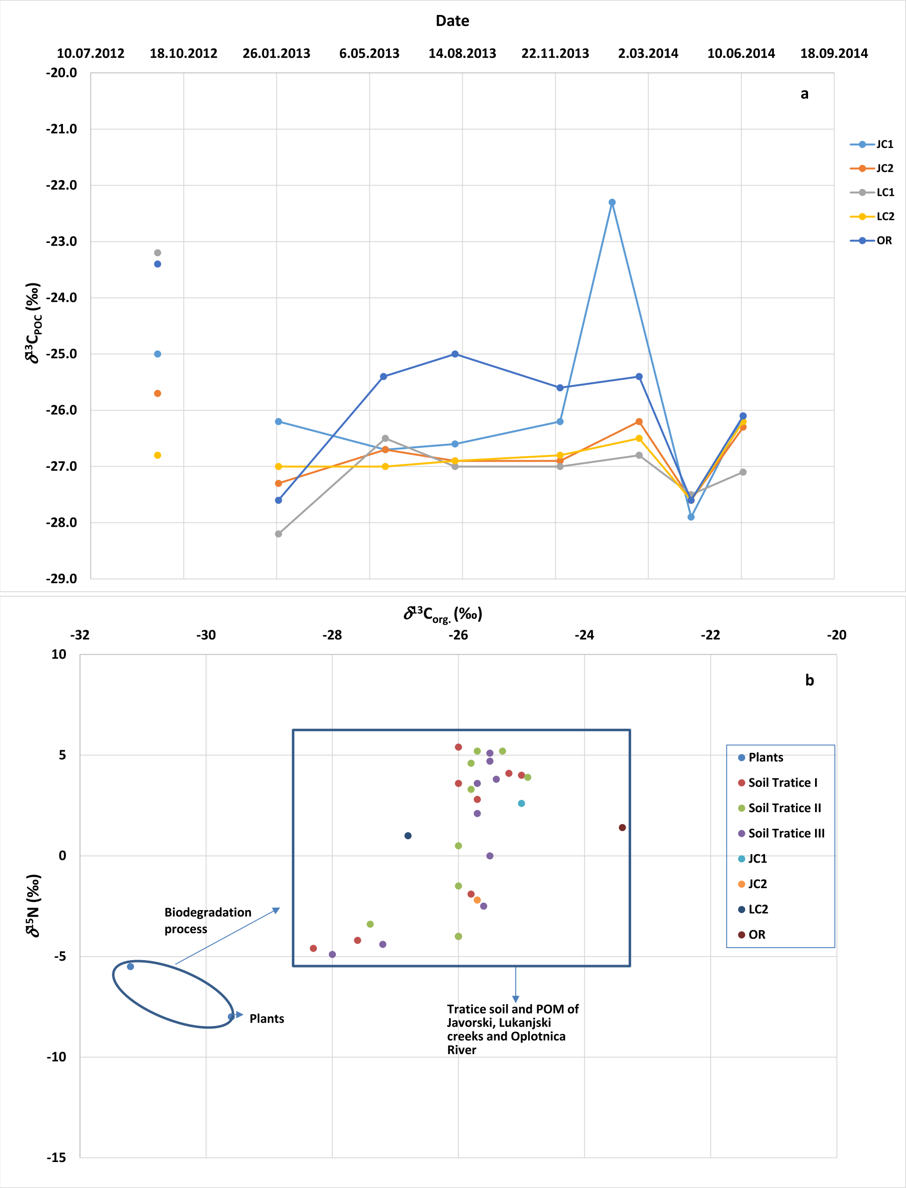

Fig. 9 **a** Temporal changes in δ^{13}C$_{POC}$ in Javorski and Lukanjski creek and the Oplotnica River **b** δ^{15}N versus δ^{13}C$_{org.}$ of leaves and needles of plants, soils at sampling locations Tratice I, II, III and POM in Javorski and Lukanjski creeks and the Oplotnica River (δ^{15}N data available only from September, 2012)

These findings provide new insights into the dynamics of DIC and $\delta^{13}C_{DIC}$ in silicate catchments, including variability in $\delta^{13}C_{DIC}$ across river and creek systems, the role of silicate weathering in carbon fluxes, CO_2 evasion from small silicate watersheds, the coupling of carbon and nitrogen cycles in river sediments, the influence of rock weathering on river chemistry, and the local and global relevance of silicate catchments.

These insights offer valuable information that enhances the global understanding of carbon and nitrogen cycles on both local and global scales.

Supplementary Information The online version contains supplementary material available at https://doi.org/10.1007/s10498-025-09439-w.

Acknowledgements The authors are grateful to Mr. Stojan Žigon for technical support and isotopic analyses, to dr. Milan Kobal and Mr. Samo Grbec for soil sampling and pedological survey, to the Programme research groups "Cycling of nutrients and contaminants in the environment, mass balances and modelling environmental processes and risk analysis" (No. P1-0143), "Geochemistry and materials"(No. P1-0195) and "Forest biology, ecology and technology" (No. P4–0107), Posdoc applied research project "Conservation of quality and quantity of water aquifers in forest land"(No. Z4-9641), and Slovenian – American bilateral project 2012-2013 (BI-US/12-13-039):"Fluid dynamics and carbon cycling in sedimentary basins: geochemical characterization, evolution of biogeochemical processes and modelling"founded by Slovenian Research and Innovation Agency.

Author contributions TK, UV, JM contributed to conceptualization. TK, UV, DŽ, TV, MV were responsible for methodology, software, formal analysis, and investigation; writing—original draft preparation was performed by TK, JM, MV, TV, DŽ, UV. Review, editing, and funding acquisition were performed by TK, JM, MV, TV, UV. JM was involved in supervision.

Funding The Slovenian Research and Innovation Agency, P1-0143, Z4-9641, P1-0195, P4-0107, University of Arizona.

Data Availability Data related to current study are available: Kanduč T., Žigon S., Žlindra D., Vilhar U., McIntosh J. (2024) Data of monitoring the Oplotnica River silicate catchment (Slovenia) using stable carbon and nitrogen isotopes. https://doi.org/10.17632/gbt7swp999.1.

Declarations

Competing interests The authors declare no competing interests.

References

Altherr R, Lugovic B, Meyer HP, Majer V (1995) Early Miocene post-collisional calc-alkaline magmatism along the easternmost segment of the periadriatic fault system (Slovenia and Croatia). Mineral Petrol 54:225–247

Amiotte Suchet P, Probst JL (1993) Modelling of atmospheric CO_2 consumption by chemical weathering of rocks: application to the Garonne, Congo and Amazon basins. Chem Geol 107:205–210

Atekwana EA, Fonyuy EW (2009) Dissolved inorganic carbon concentrations and stable carbon isotope ratios in streams polluted by variable amounts of acid mine drainage. J Hydrol 372:136–148. https://doi.org/10.1016/j.jhydrol.2009.04.010

Atekwana EA, Molwalefhe L, Kgovadi O, Cruse AM (2016) Effect of evapotranspiration on dissolved inorganic carbon and stable carbon isotopic evolution in rivers in semi-arid climates: The Okavango Delta in North West Botswana. J Hydrol: Reg Stud 7:1–13

Aucour AM, Sheppard SMF, Guyomar O, Wattelet J (1999) Use of ^{13}C to trace origin and cycling of inorganic carbon in the Rhone River system. Chem Geol 159:87–105

Berner RA, Lasaga AC, Garrels RM (1983) The carbonate-silicate geochemical cycle and its effect on atmospheric carbon dioxide over the past 100 million years. Am J Sci 283:641–683. https://doi.org/10.2475/ajs.283.7.641

Berner EK, Berner RA (1996) Global Environment: Water, Air and Geochemical cycles. In: Handbook of Soil Science. Edited by Sumner M. E., New York: Prentice Hall, Upper Saddle River, pp. 376.

Broecker WS (1974) Chemical oceanography. In: Leeder MR (ed) Sedimentology and sedimentary basins. Harcout-Brace-Jovanovich, New York, p 592

Broecker HC, Peterman J, Siems W (1978) The influence of wind on CO_2–exchange in a wind–wave tunnel, including the efects of monolayers. J Mar Res 36:595–610

Brouwer C, Goffeau A, Heibloem M (1985) Irrigation Water Management: Training Manual No. 1 – Introduction to Irrigation. Rome, Food and Agriculture Organization of the United Nations, 152 p.

Clark I, Fritz P (1997) Environmental isotopes in hydrogeology. Lewis Publishers, New York, p 326

da Conceiçao T, Fabiano AM, Fernandes RB, Moruzzi JM (2024) Dynamics of dissolved inorganic carbon (DIC) and stable C isotope ratios ($\delta^{13}C_{DIC}$) in a tropical watershed with diversified land use in São Paulo State, Brazil. Sci Total Environ 933:173071

Derrien M, Kim M, Ock G, Hong S, Cho J, Shin KM, Hur J (2018) Estimations of different contributions to sediment organic matter in an agricultural-forested watershed using end member mixing analysis based on stable isotope ratios and fluoroscence spectroscopy. Sci Total Environ 618:569–578

Fodor LI, Gerdes A, Dunkl I, Koroknai B, Pécskay Z, Trajanova M, Horváth P, Vrabec M, Jelen B, Balogh K, Frisch W (2008) Miocene emplacement and rapid cooling of the Pohorje pluton at the Alpine-Pannonian-Dinaridic junction, Slovenia. Swiss J Geosci 101(S1):255–271. https://doi.org/10.1007/s00015-008-1286-9

Fonyuy EW, Atekwana EA (2008) Dissolved inorganic carbon evolution and stable carbon isotope fractionation in acid mine drainage contaminated streams: Insights from a laboratory study. Appl Geochem 23:2634–2648

Gaillardet J, Dupre B, Allegre CJ (1999) Geochemistry of large river suspended sediments: silicate weathering or recycling tracer? Geochim Cosmochim Acta 63:4037–1051

Guo Q, Wang C, Wei R, Zhu G, Cui M, Okolic CP (2020) Qualitative and quantitative analysis of source for organic carbon and nitrogen in sediments of rivers and lakes based on stable isotopes. Ecotoxicol Environ Saf 195:110436

Holley EH (1977) Oxygen transfer at the air–water interface. In: Gibbs RJ (ed) Transport processes in lakes and oceans, Proceedings Symposium On Transport. Processes in the Ocean held at the 2nd Nat. Meet Of the AICE, Atlantic City, N. J. Aug. 29.–Sep. 1, 1976, pp 117–150.

http://ksh.fgg.uni-lj.si/ewnsi/enwnsi-eng.htm(online document)

https://gis.arso.gov.si/atlasokolja/profile.aspx?id=Atlas_Okolja_AXL@Arso(online document)

https://www.windfinder.com/forecast/oplotnica_oplotnica_slovenia(online document)

Huang C, Chen F, Zhang S, Chen C, Meng Y, Zhu Q, Song Z (2020) Carbon and nitrogen isotopic composition of particulate organic matter in the Pearl River estuary and the adjacent shelf. Estuarine, coastal and shelf science 246: 107003. https://sl.wikipedia.org/wiki/Oplotni%C5%A1%C4%8Dica#cite_note-22, accessed 24. September, 2024.

ISO 10304–1 (2007) Water quality—Determination of dissolved anions by liquid chromatography of ions; Part 1: Determination of bromide, chloride, fluoride, nitrate, nitrite, phosphate and sulfate. International Organization for Standardization, Geneva, Switzerland, 11 p.

ISO 10390 (2005) Soil quality—Determination of pH. International Organization for Standardization, Geneva, Switzerland, 7 p.

ISO 10523 (2008) Water quality—Determination of pH. International Organization for Standardization, Geneva, Switzerland, 13 p.

ISO 10693 (1995) Soil quality—Determination of carbonate content — Volumetric method. International Organization for Standardization, Geneva, Switzerland, 7 p.

ISO 11277:1998/Cor 1: (2002) Soil quality—Determination of particle size distribution in mineral soil material—Method by sieving and sedimentation. International Organization for Standardization, Geneva, Switzerland, 30 p, 2 p.

ISO 11464 (2006) Soil quality—Pretreatment of samples for physico-chemical analysis. International Organization for Standardization, Geneva, Switzerland, 11 p.

ISO 13878 (1998) Soil quality—Determination of total nitrogen content by dry combustion ("elemental analysis"). International Organization for Standardization, Geneva, Switzerland, 5 p.

ISO 14911 (1998) Water quality — Determination of dissolved Li^+, Na^+, NH_4^+, K^+, Mn^{2+}, Ca^{2+}, Mg^{2+}, Sr^{2+} and Ba^{2+} using ion chromatography—Method for water and waste water. International Organization for Standardization, Geneva, Switzerland, 18 p.

ISO 7888 (1985) Water quality—Determination of electrical conductivity. International Organization for Standardization, Geneva, Switzerland. 6 p.

ISO 8245 (1999) Water quality—Guidelines for the determination of total organic carbon (TOC) and dissolved organic carbon (DOC). International Organization for Standardization, Geneva, Switzerland, 11 p.

ISO 9963–1 (1994) Water quality—Determination of alkalinity; Part 1: Determination of total and composite alkalinity. International Organization for Standardization, Geneva, Switzerland, 6 p.

SIST ISO 11465 (1993) Soil quality — Determination of dry matter and water content on a mass basis — Gravimetric method. International Organization for Standardization, Geneva, Switzerland, 3 p.

Jähne B, Heinz G, Dietrich W (1987) Measurements of the diffusion coefficients of sparingly soluble gases in water. J Geophys Res 92:10767–10776

Janäk M, Cornell D, Froitzheim N, De Hoog JCM, Broska I, Vrabec M, Hurai V (2009) Eclogite-hosting metapelites from the Pohorje Mountains (Eastern Alps): P-T evolution, zircon geochronology and tectonic implications. Eur J Mineral 21:1191–1212. https://doi.org/10.1127/0935-1221/2009/0021-1966

Juhlke TR, Geldern RV, Huneau F, Garel E, Santoni S, Hermmerle H, Barth JAC (2019) Riverine carbon dioxide evasion along a high-relief watercourse derived from seasonal dynamics of the water-atmosphere gas exchange. Sci Total Environ 657:1311–1322. https://doi.org/10.1016/j.scitotenv.2018.12.158

Kanduč T, Szramek K, Ogrinc N, Walter LM (2007a) Origin and cycling of riverine inorganic carbon in the Sava River watershed (Slovenia) inferred from major solutes and stable isotopes. Biogeochemistry 86:137–154

Kanduč T, Ogrinc N, Mrak T (2007b) Characteristics of suspended matter in the River Sava watershed, Slovenia. Isot Environ Health Stud 43(4):369–285

Kanduč T, Kocman D, Ogrinc N (2008) Hydrogeochemical and stable isotope characteristics of the river Idrijca (Slovenia), the boundary watershed between Adriatic and Black Seas. Aquat Geochem 14:239–262. https://doi.org/10.1007/s10498-008-9335-2

Kanduč T, Burnik Šturm M, McIntosh J (2013) Chemical dynamics and evolution of biogeochemical processes in alpine river Kamniška Bistrica North Slovenia. Aquatic Geochem 19:323–346. https://doi.org/10.1007/s110498-013-9197-4

Kanduč T, Geršl M, Geršlová E, McIntosh J (2023) Temporal and seasonal variations of silicate Svratka River and sediment characterization Czech Republic: geochemical and stable isotope approach. Aquatic Geochem 29:145–171

Kanduc T et al (2014) A geochemical and stable isotope investigation of groundwater/surface-water interactions in the Velenje Basin, Slovenia. Hydrogeol J 22:971

Kanduč T, Žigon S, Žlindra D, Vilhar U, McIntosh J (2024) Data of monitoring the Oplotnica River silicate catchment (Slovenia) using stable carbon and nitrogen isotopes. https://doi.org/10.17632/gbt7swp999.1

Kendall C, Silva SR, Kelly VJ (2001) Carbon and nitrogen isotopic compositions of particulate organic matter in four large river systemsacross the United States. Hydrol Process 15(7):1301–1346

Krajnc B, Fujiyoshi R, Vaupotič J, Amano H, Sakuta Y, Gregorič A, Ogrinc N (2016) Using ^{222}Rn and carbon isotopes (^{12}C, ^{13}C and ^{14}C) to determine CO_2 sources on forest soils developed on contrasting geology in Slovenia. Environ Earth Sci 75:1068. https://doi.org/10.1007/s12665-016-5866-0

Krusche AV, Martinelli LA, Vistoria RL, Bernardes M, Camargo PB, Ballester MV, Trumbore SE (2002) Composition of particulate and dissolved organic matter in a disturbed watershed od Southeast Brazil (Piracicaba River basin). Water Res 36:2743–2752. https://doi.org/10.1016/S0043-1354(01)00495-X

Lan X, Tans P, Thorning KW (2024) Trends in globally –averaged CO_2 determined from NOAA Global Monitoring Laboratory measurements. Version Tuesday, 05-Nov-2024 13: 17:54 MST, https://doi.org/10.15138/9NOH-ZHO7.

Lavtar K, Bezak N (2020) Šraj M (2020) Rainfall-runoff modeling of the Nested Non-Homogenous Sava River sub-catchments in Slovenia. Water 12(1):128. https://doi.org/10.3390/w12010128

Li Z, Li X, Wang X, Ma J, Xu J, Xu X, Han R, Zhou Y, Yan X, Wang G (2020) Isotopic evidence revealing spatial heterogenity for source composition of sedimentary organic matters in taihu lake. China Ecol Indic 109:105854

Lu F, Liu Z, Ji H (2012) Carbon and nitrogen isotopes analysis and sources of organic matter in the upper reaches of the Chaobai river nera Beijing China. Sci China Earth Sci 56(2):217–237 ((**in Chinese**))

Ludwig W, Amiotte-Suchet P, Probst JL (1996a) River discharges of carbon to the world's oceans: determining local inputs of alkalinity and of dissolved and particulate organic carbon. C. R. Acad Sci Ser Iia: Sci Terre Planetes 323:1007–1014

Ludwig W, Probst JL, Kempe S (1996b) Predicting the oceanic input of organic carbon by continental erosion. Global Biogeochem Cycles 10:23–41. https://doi.org/10.1029/95GB02925

Mayorga E, Aufdenkampe AK, Masiello CA, Krusche AV, Hedges JI, Quay PD, Richey JE, Brown TA (2005) Young organic matter as a source of carbon dioxide outgassing from Amazonian rivers. Nature 436:538–541

Mioč P, Žnidarčič M (1977) Osnovna geološka karta SFRJ. L 33–55, Slovenj Gradec. [Kartografsko gradivo]. Beograd: Zvezni geološki zavod. (in Slovene)

Mioč P (1978) Tolmač za list Slovenj Gradec: L 33–55: Socialistična fegerativna republika Jugoslavija, osnovna geološka karta, 1:100000, Zvezni geološki zavod, 74 str. (in Slovene)

Mook WG, Tan FC (1991) Stable carbon isotopes in rivers and estuaries. In: Degens ET, Kempe S, Ridley JE (eds) Biogeochemistry of major world rivers. Wiley, New York, pp 245–264

Mook WG (1970) Stable carbon and oxygen isotopes of natural waters in the Netherlands, Isotope Hydrology, IAEA, Vienna, 163–190.

Ogawa Y, Okomoto Y, Sadoba RB, Kanzaki M (2021) Sediment organic matter source estimation and ecological classification in the semi-enclosed Bata bay Estuary Phillippines. Int J Sediment Res 36(1):110–119

Ogrinc N, Kanduč T, Krajnc B, Vilhar U, Simončič P, Lixin J (2016) Inorganic and organic dynamics in forested soils developed on contrasting geology in Slovenia- a stable isotope approach. J Soils Sediments: Prot, Risk Assess Remediat 16(2):382–395

Parkhurst DL, Appelo CAJ (1999) User's guide to PHREEQC (version 2)—a computer program for speciation, batch-reaction, one-dimensional transport, and inverse geochemical calculations. WaterResources Investigations Report 99–4259.

Poli G, Christofides G, Koroneos A, Trajanova M, Zupančič N (2020) Multiple processes in the genesis of the Pohorje igneous complex: Evidence from petrology and geochemistry. Lithos 364–365:105512–105512. https://doi.org/10.1016/j.lithos.2020.105512

Porowska D (2015) Determination of the origin of dissolved inorganic carbon in groundwater around a reclaimed landfill in Otwock using stable carbon isotopes. Waste Manage 39:216–225

Rahman A, Rathi A, Nambiar R, Mishra PK, Anoop A, Bhusan R, Kumar S (2021) Signatures of natural to anthropogenic transition in lake sediments from the central Himalaya using stable isotopes. Appl Geochem 134:105095

Raymond PA, Hartmann J, Lauerwald R, Sobek S, McDonald C, Hoover M, Butman D, Striegl R, Mayorga E, Humborg C, Kortelainen P, Dürr H, Meybeck M, Ciais P, Guth P (2013) Global carbon dioxide emissions from inland waters. Nature 503:355–359. https://doi.org/10.1038/nature12760

Ren X, Yu R, Kang J, Wang R, Li X, Wang R, Li X, Wang D, Zhang P (2024) Unraveling the sources of organic matter in suspended particulates and sediment in a closed inland lake using stable isotope fingerprinting. Int J Sedim Res 39:421–434

Roulet N, Moore TM (2006) Browning the waters. Nature 444(16):283–284

Schuster PF, Reddy MM (2005) Particulate carbon (PC) and particulate nitrogen (PN). Water and sediment quality in the Yukan River Basin, Alaska, during water year 2001. Open-File Report 03–427, National Research Programm USGS. Available online at: http://pubs.usgs.gov/org/2003/ofr03427, assessed 1. September 2005

Senarathne S, van Geldern R, Chandrajith R, Barth JAC (2024) Unexpected contributions by carbonates and organic matter in a silicate-dominated tropical catchment: an isotope approach. Sci Total Environ 20(948):174651

Staddon PL (2004) Carbon isotopes in functional soil ecology. *Trends in Ecology & Evolution, 19*(3), 148–154. https://doi.org/10.1016/j.tree.2003.12.003

Stumm W, Morgan JJ (1981) Aquatic Chemistry: An Introduction Emphasizing Chemical Equilibria in Natural Waters Equilibria, 2nd edn. John Wiley & Sons Inc, New Jersey

Szramek K, McIntosh JC, Williams EL, Kanduc T, Ogrinc N, Walter LM (2007) Relative weathering intensity of calcite versus dolomite in carbonate-bearing temperate zone watersheds: carbonate geochemistry and fluxes from catchments within the St. Lawrence and Danube river basins. Geochem Geophys Geosyst. https://doi.org/10.1029/2006GC001337

Tang Y, Zhang G (2010) Identifying sources of particles organic matter in surface water based on stable isotope tracing on basin scale. China Environ Sci 30(9):1257–1267 ((**in Chinese**))

Tao S (1998) Spatial and temporal variation in DOC in the Yichun River, China. Water Res 32:2205–2210

Thompson HA, White JR, Pratt LM (2018) Spatial variation in stable isotopic composition of organic matter of macrophytes and sediments from a small arctic lake in West Greenland. Arctic Antartctic Alpine Res 50(1):S100017

Thöni M (2002) Sm–Nd isotope systematics in garnet from different lithologies (Eastern Alps): age results and an evaluation of potential problems for garnet Sm–Nd chronometry. Chem Geol 185:255–281

Tian M, Yang X, Ran L, Su Y, Li L, Yu R, Hu H, Xi LuX (2019) Impact of land cover types on riverine CO_2 outgassing in the Yellow River source region. Water 11(11):2243. https://doi.org/10.3390/w11112243

Trajanova M, Pecskay Z, Itaya T (2008) K-Ar geochronology and petrography of the miocene pohorje mountains batholith (Slovenia). Geol Carpath 59(3):247–260

Uher P, Janak M, Konecny P, Vrabec M (2014) Rare-element granitic pegmatite of Miocene age emplaced in UHP rocks from Visole, Pohorje Mountains (Eastern Alps, Slovenia): Accessory minerals, monazite and uraninite chemical dating. Geologica Carpathica 65(2):131–146. https://doi.org/10.2478/geoca-2014-0009

USDI (2001) Water measurement manual. U. S. Department of the Interior Bureau of Reclamation, Washington, p 317

Vilhar U, Kestnar K, Vidmar A, Šraj M (2015) Measuring and modelling of runoff from two forested watersheds in Pohorje. Acta Hydrotechnica 28(48):49–64

Vilhar U, Kutnar L, Urbančič M, Simončič P (2016) Mikrorastiščne razmere kot pomemben dejavnik premene smrekovih monokultur na bukovih rastiščih. Microsite conditions as a major factor in the coversion of spruce monocultures on beech sites. Gozdarski Vestnik 74:59–72

Walker JCG, Hays PB, Kasting JF (1981) A negative feedback mechanism for the long-term stabilization of Earth's surface temperature. J Geophys Res 86:9776–9782. https://doi.org/10.1029/JC086iC10p09776

Wang W, Li SL, Zhong J, Li C, Yi Y, Chen S, Ren Y (2019) Understanding transport and transformation of dissolved inorganic carbon (DIC) in the reservoir system using $\delta^{13}C_{DIC}$ and water chemistry. J Hydrol 574:193–201. https://doi.org/10.1029/j.hydrol.2019.04.036

Yang C, Telmer K, Veizer J (1996) Chemical dynamics of the St. Laurence“ riverine system”: δD_{H2O}, $\delta^{18}O_{H2O}$, $\delta^{13}C_{DIC}$, δ^{34}Ssulfate, and dissolved $^{87}Sr/^{86}Sr$. Geochim Cosmochim Acta 60:851–866. https://doi.org/10.1016/0016-7037(95)00445-9

Yang W, Zhou M, Shen H, Wang Z, Li W (2020) Organic carbon and nitrogen isotopes of lakes in cold and arid region during the frozen period. China Environ Sci 40(2):789–797 ((**in Chinese**))

Zou J (2016) Sources and dynamics of inorganic carbon within the upper reaches of the Xi River Basin Southwest China. PLoS ONE 11(8):e0160964. https://doi.org/10.1371/journal.pone.0160964

Authors and Affiliations

Tjaša Kanduč[1] · **Mirijam Vrabec**[2] · **Timotej Verbovšek**[2] · **Jennifer McIntosh**[3] · **Daniel Žlindra**[4] · **Urša Vilhar**[4]

✉ Tjaša Kanduč
tjasa.kanduc@ijs.si

Mirijam Vrabec
mirijam.vrabec@ntf.uni-lj.si

Timotej Verbovšek
timotej.verbovsek@ntf.uni-lj.si

Jennifer McIntosh
jenmc@arizona.edu

Daniel Žlindra
daniel.zlindra@gozdis.si

Urša Vilhar
ursa.vilhar@gozdis.si

[1] Department of Environmental Sciences, Jožef Stefan Institute, Jamova Cesta 39, 1000 Ljubljana, Slovenia

[2] Faculty of Natural Sciences and Engineering, University of Ljubljana, Aškerčeva 12, 1000 Ljubljana, Slovenia

[3] Department of Hydrology and Atmospheric Sciences, University of Arizona, 1133 E. James E, Rogers Way, Tucson, AZ 85721, USA

[4] Department of Forest Ecology, Slovenian Forestry Institute, Večna Pot 2, 1000 Ljubljana, Slovenia